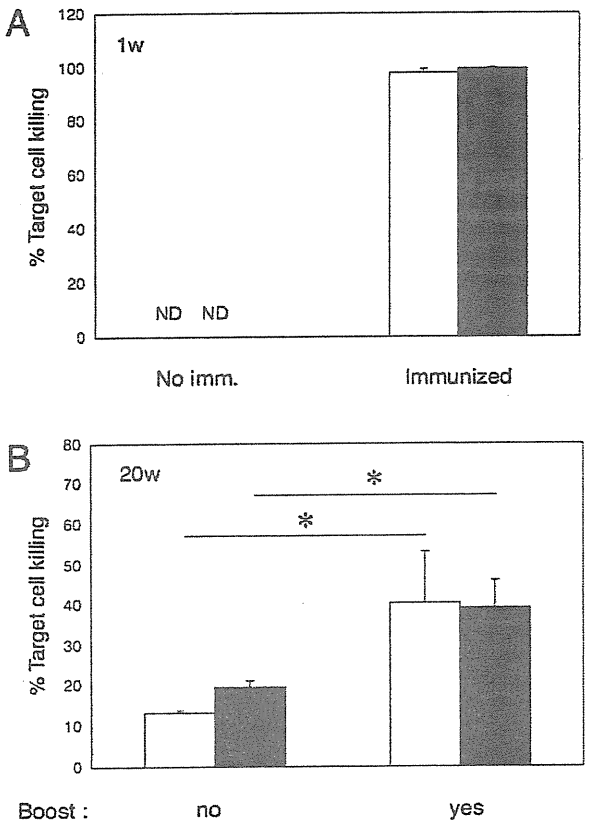

Figure 5. Effect of *in vivo* elimination of $CD4^+$ T cells on the induction of primary and secondary CTL responses by $OVA_{257-264}$-liposomes. Mice with (closed box) or without (open box) $CD4^+$ T-cell elimination were immunized with 50 μl of $OVA_{257-264}$-liposome solution in the presence of 5 μg CpG, and CTL induction was monitored. A, CTL response 1 week after immunization. B, CTL response 20 weeks after immunization with or without booster injection. *In vivo* CTL assay was performed 3 days after the booster injection. Data represent mean percent killing and SE of three mice per group. ND, not detected. *, significant difference ($p>0.01$).
doi:10.1371/journal.pone.0015091.g005

The potential usefulness of surface-linked liposomal antigens for application to vaccine development was further investigated. During the course of this investigation, a significant difference was observed in the recognition of liposomal antigens by antigen-presenting cells (APCs) between liposomes with different lipid components [23], and this difference was closely correlated with the adjuvant activity of liposomes [24]. In addition to this "quantitative" difference between liposomes with different lipid components, a "qualitative" difference (i.e., different abilities to induce cross-presentation) was also observed between liposomes with different lipid components [17]. Although the precise mechanism underlying this difference is currently unclear, the significant difference in membrane mobility observed between these liposomes [24] might affect their ability to induce cross-presentation. Thus, by utilizing their ability to induce cross-presentation, surface-linked liposomal antigens could be used to develop virus vaccines that induce a cytotoxic T-cell (CTL) response, as well as tumor vaccine preparations that present tumor antigens to APCs and induce effective antitumor responses [18].

Regarding the necessity of $CD4^+$ T cells in the generation of memory $CD8^+$ T cells, the results of the present study differed from those reported previously [1-5]. The difference in these findings may be due to differences in how mice were primed with antigens; in most of the studies reported previously, mice were primed by infecting viruses, such as LCMV [1,3,5], H3N2 influenza virus [2], and recombinant vaccinia virus [4], whereas in the present study, mice were immunized with OVA-derived CTL epitope peptides. Perhaps the difference in the requirements of $CD4^+$ T cells observed among those studies [1–5] and the present study was due to the difference in the efficiency of inducing the presentation of the immunodominant CTL epitope by APCs. In general, only ~1/2000 of the peptides in a foreign antigen expressed by an appropriate APC achieve immunodominant status with a given class I allele [25]. However, in the present study, immunization with $OVA_{257-264}$-liposome successfully induced both primary and secondary CTL responses without the presence of $CD4^+$ T cells (Figures 2 to 5). In addition, it was reported previously that antigens coupled to the surface of liposomes are recognized effectively by APCs and presented to T cells [24]. Therefore, although the TLR-ligand (CpG, in the present study) was necessary to mimic viral infection in order to induce CTL responses in the immunization with liposome-coupled peptides, $CD4^+$ T cells were not required for the induction and maintenance of $CD8^+$ memory T cells.

There is considerable interest in developing vaccines that elicit effective antiviral $CD8^+$ T cell responses [26] against a variety of viruses, such as HIV [27], HCV [28], and SARS coronavirus [29]. For this purpose, the utilization of the immunodominant CTL epitope would be more effective than the use of an attenuated, inactivated, or subunit vaccine in the development of virus vaccines to elicit effective antiviral $CD8^+$ T cell responses. For example, although the risk of a major global pandemic of avian influenza has created widespread concern, vaccines designed to induce antibodies against H5 haemagglutinin are expected to possess little or no efficacy, given the high rate of diversification of H5N1 strains due to the antigenic drift caused by point mutation of genes [30–33]. On the other hand, it is known that cytotoxic T cells specific for the internal proteins NP and M1 show high cross-reactivity between strains and between subtypes, reflecting high conservation of the internal proteins [34–37]. In addition, Lee et al. [38] recently reported that people who have not been exposed to H5N1 viruses have cross-reactive $CD8^+$ T cell memory to a wide range of H5N1 peptides. Therefore, these peptides are expected to be used to add a $CD8^+$ T cell component to current antibody-focused vaccine strategies with a view to reducing the impact of infection with novel influenza A viruses [39]. Epstein et al. [40] studied DNA vaccination in mice with plasmids expressing conserved nucleoprotein (NP) and matrix (M) from an H1N1 virus. However, the DNA vaccination alone protected poorly against a highly virulent strain of H5N1 influenza viruses.

Recently, we reported that peptides derived from the internal NP protein of the H3N2 influenza virus, chemically coupled to the surface of liposomes, induced antigen-specific CTLs and successfully inhibited the growth of H3N2 influenza virus in the lung [41]. More recently, we determined human HLA class I-restricted, immunodominant CTL epitopes derived from internal proteins of H5N1 influenza viruses [42]. Similar to those results reported previously [34–37,43], most of the CTL epitopes determined were well conserved and were identical with those involved in H1N1 and H3N2 influenza viruses. The combined use of these CTL epitope peptides, common to influenza viruses, and the surface-linked liposomal antigens which induce long-lived memory $CD8^+$ T cells without $CD4^+$ T cell help, was demonstrated to be

applicable for the development of a CTL-based influenza vaccine that is capable of inducing protection against heterosubtypic influenza viruses [42].

Taken together, these results suggest that surface-linked liposomal antigens might be applicable for the development of CTL-based vaccines to induce long-term prevention against infection with viruses other than influenza viruses, especially for those viruses that evade humoral immunity by varying their surface proteins, such as HIV, HCV, and SARS coronaviruses.

Materials and Methods

Mice

CBF1 mice (5–6 wk of age) were purchased from SLC (Shizuoka, Japan). All mice were maintained under specific pathogen-free conditions. Experiments in the present study were approved (permit numbers 208021 and 209082) by the Animal Research Committee of National Institute of Infectious Diseases, Tokyo, Japan and the mice were handled according to international guidelines for experiments with animals.

Chemicals

All phospholipids were obtained from NOF Co. (Tokyo, Japan). Reagent grades of cholesterol were purchased from Wako Pure Chemicals (Osaka, Japan).

Antigens and Reagents

Ovalbumin (OVA, grade VII) was purchased from Sigma-Aldrich. Mouse MHC class-I (K^b)-binding peptides $OVA_{257-264}$ (SIINFEKL) were obtained from Operon Biotechnologies (Tokyo, Japan). Synthetic CpG ODN (5002: TCCATGACGTTCTT-GATGTT), phosphorothioate-protected to avoid nuclease-dependent degradation, was purchased from Invitrogen.

Liposomes

The liposomes used in this study are provided by NOF corporation (Tokyo, Japan). They consisted of dioleoyl phosphatidylcholine (DOPC), dioleoyl phosphatidyl ethanolamine (DOPE), dioleoyl phosphatidyl glycerol (DOPG), and cholesterol in a 4:3:2:7 molar ratio. The crude liposome solution was passed through a membrane filter (Nucleopore polycarbonate filter; Coster) with a pore size of 0.2 μm.

Coupling of OVA peptides to liposomes

Liposomal conjugates with OVA peptides were prepared essentially in the same way as described previously [17] via disuccinimidyl suberate (DSS). Briefly, a mixture of 10 ml of anhydrous chloroform solution containing 0.136 mM DOPE and 24 μl of TEA was added in drops to 26.6 ml of anhydrous chloroform solution containing 0.681 mM DSS and stirred for 5 h at 40°C. The solvent was evaporated under reduced pressure, and 18 ml of a 2:1 mixture of ethyl acetate and tetrahydrofuran was added to dissolve the residue. Then, 36 ml of 100-mM sodium phosphate (pH 5.5) and 90 ml of saturated NaCl aqueous solution were added to the solution, shaken for 1 min, and allowed to separate. To remove undesirable materials, the upper layer was washed with the same buffer and, after evaporation of the solvent, 3 ml of acetone was added to dissolve the residue. One hundred ml of ice-cold acetone was added in drops and kept on ice for 30 min to precipitate. Crystals were collected and dissolved in 5 ml of chloroform. After evaporation, 34.4 mg of DOPE-DSS was obtained. Then, 0.18 mM DOPC, 0.03 mM DOPE-DSS, 0.21 mM cholesterol, and 0.06 mM DOPG were dissolved in 10 ml of chloroform/methanol. The solvent was removed under reduced pressure and 5.8 ml of phosphate buffer (pH 7.2) was added to make a 4.8% lipid suspension. The vesicle dispersion was extruded through a 0.2-μm polycarbonate filter to adjust the liposome size. A 2-ml suspension of DSS-introduced liposome and 0.5 ml of 5-mg/ml OVA peptide solution were mixed and stirred for 3 days at 4°C. The liposome-coupled- and uncoupled peptides were separated as described above using CL-4B column chromatography. The resulting solution of $OVA_{257-264}$-liposome conjugates contained 47 μg/ml of peptides as assessed by amino-acid quantitative analysis done by Toray Research Center (Kanagawa, Japan).

Immunization

All the mice were immunized with indicated doses of $OVA_{257-264}$-liposome conjugates via subctaneous injection in the presence of 5 μg/mouse CpG. For the booster immunization, the mice were immunized intraperitoneally (ip) with 200 μl of 1-mg/ml OVA in PBS solution.

In vivo elimination of $CD4^+$ T cells

For the *in vivo* elimination of $CD4^+$ T cells, mice received weekly ip injection with 0.5 mg of GK1.5, a monoclonal anti-CD4 antibody, throughout the experimental period. This treatment resulted in a >99% decrease in the number of $CD4^+$ T cells in the spleen and lymph nodes as determined by fluorescence-activated cell sorter (FACS) analysis.

In vivo cytotoxicity assay

Spleen cells of naive CBF1 mice were labeled with either 0.5 μM (dull) or 5 μM (bright) CFSE for 15 min at 37°C using a Cell Trace CFSE cell proliferation kit (Molecular Probes, Eugene, OR) and washed twice with ice-cold PBS. CFSE-bright cells were subsequently pulsed with 0.5 μg/ml of $OVA_{257-264}$ for 90 min at 37°C. CFSE-bright cells and CFSE-dull cells were mixed at a 1:1 ratio, and then a total of 1×10^6 cells was injected i.v. into the indicated group of mice. Twenty hours later, spleen cells were harvested from each mouse and analyzed by using FACSCalibur (Becton Dickinson, Mountain View, CA).

Cell culture

All incubations were performed in RPMI-1640 (Invitrogen Life Technologies) supplemented with 10% heat-inactivated FCS (HyClone), 100 U/ml penicillin, and 100 μg/ml streptomycin (Invitrogen).

Preparation of dendritic cells (DC) and $CD8^+$ T cells

DCs and $CD8^+$ T cells were obtained from spleen cells of CBF1 mice using the magnetic cell sorter system MACS according to the manufacturer's protocol using anti-CD11c and anti-CD8 antibody-coated microbeads (Miltenyi Biotec), respectively. $CD8^+$ T cells and DCs were suspended in RPMI-1640 containing 10% FCS at cell densities of 2×10^6/ml and 8×10^5/ml, respectively. The $CD8^+$ T cell suspension was plated at 250 μl per well onto 48-well culture plates (No. 3047; BD Biosciences), and 250 μl of DC suspension and 500 μl of 40 μM $OVA_{257-264}$ solution in the same medium were added to the plates. After incubation in a CO_2 incubator for 5 days, the culture supernatants were collected and assayed for the concentration of IFN-γ.

Cytokine assays

IFN-γ in the culture supernatant was measured using the Biotrak mouse ELISA system (GE Healthcare, UK). All test samples were assayed in duplicate, and the SE in each test was always less than 5% of the mean value.

T cell proliferation assay

Splenic $CD8^+$ T cells (5×10^5 cells/well) of immunized mice and whole spleen cells (1×10^5 cells/well) of 25 Gy-irradiated naïve mice were cultured in 96-well plates for 4 days in the presence (closed box) or absence (open box) of 20 μM OVA. The cells were pulsed with 1.25 μCi (0.046 MBq) [^{3}H]-thymidine (PerkinElmer) for the final 6 hours of the culture, and, after harvesting, cell proliferation was monitored using TopCount (PerkinElmer).

Statistical analysis

Student's *t* test was employed for the statistical analysis.

Author Contributions

Conceived and designed the experiments: TU. Performed the experiments: MT YT TK. Analyzed the data: MT TU. Contributed reagents/materials/analysis tools: MT YT. Wrote the paper: TU. N/A.

References

1. Matloubian M, Concepcion RJ, Ahmed R (1994) $CD4^+$ T cells are required to sustain $CD8^+$ cytotoxic T-cell responses during chronic viral infection. J Virol 68: 8056–8063.
2. Belz GT, Wodartz D, Diaz G, Nowak MA, Doherty PC (2002) Compromised influenza virus-specific $CD8^+$-T-cell memory in $CD4^+$-T-cell-deficient mice. J Virol 76: 12388–12393.
3. Janssen EM, Lemmens EE, Wolfe T, Christen U, von Herrath MG, et al. (2003) $CD4^+$ T cells are required for the secondary expansion and memory in $CD8^+$ T lymphocytes. Nature 421: 852–856.
4. Shedlock DJ, Shen H (2003) Requirement for CD4 T cell help in generating functional CD8 T cell memory. Science 300: 337–339.
5. Sun JC, Williams MA, Bevan MJ (2004) $CD4^+$ T cells are required for the maintenance, not programming, of memory $CD8^+$ T cells after acute infection. Nat Immunol 5: 927–933.
6. Bennett SR, Carbone FR, Karamalis F, Flavell RA, Miller JF, et al. (1998) Help for cytotoxic-T-cell responses is mediated by CD40 signaling. Nature 393: 478–480.
7. Bourgeois C, Rocha B, Tanchot C (2002) A role for CD40 expression on $CD8^+$ T cells in the generation of $CD8^+$ T cell memory. Science 297: 2060–2063.
8. Lee BO, Hartson L, Randall TD (2003) CD40-deficient, influenza-specific CD8 memory T cells develop and function normally in a CD40-sufficient environment. J Exp Med 198: 1759–1764.
9. Sun JC, Bevan MJ (2004) Long-lived CD8 memory and protective immunity in the absence of CD40 expression on CD8 T cells. J Immunol 172: 3385–3389.
10. Hernandez MG, Shen L, Rock KL (2007) CD40-CD40 ligand interaction between dendritic cells and $CD8^+$ T cells is needed to stimulated maximal T cell responses in the absence of $CD4^+$ T cell help. J Immunol 178: 2844–2852.
11. Heath WR, Carbone FR (2001) Cross-presentation, dendritic cells, tolerance and immunity. Annu Rev Immunol 19: 47–64.
12. Glenny AT, Pope CG (1926) Immunology notes. XXIII. The antigenic value of toxoid precipitated by potassium alum. J Pathol Bacteriol 29: 31–40.
13. Aggrebeck H, Wantzin J, Heon I (1996) Booster vaccination against diphtheria and tetanus in man: comparison of three different vaccine formations-III. Vaccine 14: 1265–1272.
14. Petrovsky N (2006) Novel human polysaccharide adjuvants with dual Th1 and Th2 potentiating activity. Vaccine 24 S2: 26–29.
15. Khajueia A, Gupta A, Singh S, Malik F, Singh J, et al. (2007) A new plant based vaccine adjuvant. Vaccine 25: 2706–2715.
16. Sun Y, Liu J (2008) Adjuvant effect of water-soluble polysaccharide (PAP) from the mycelium of Polyporus albicans on the immune responses to ovalbumin in mice. Vaccine 26: 3932–3936.
17. Taneichi M, Ishida H, Kajino K, Ogasawara K, Tanaka Y, et al. (2006) Antigens chemically coupled to the surface of liposomes are cross-presented to $CD8^+$ T cells and induce potent antitumor immunity. J Immunol 177: 2324–2330.
18. Uchida T, Taneichi M (2008) Clinical application of surface-linked liposomal antigens. Mini-Rev Med Chem 8: 184–192.
19. Naito S, Horino A, Nakayama M, Nakano Y, Nagai T, et al. (1996) Ovalbumin-liposome conjugate induces IgG but not IgE antibody production. Int Arch Allergy Immunol 109: 223–228.
20. Nakano Y, Mori M, Nishinohara S, Takita Y, Naito S, et al. (1999) Antigen-specific, IgE-selective unresponsiveness induced by antigen-liposome conjugates: comparison of four different conjugation methods. Int Arch Allergy Immunol 120: 199–208.
21. Taneichi M, Naito S, Kato H, Tanaka Y, Mori M, et al. (2002) T cell-independent regulation of IgE antibody production induced by surface-linked liposomal antigen. J Immunol 169: 4246–4252.
22. Uchida T (2003) Surface-linked liposomal antigen induces IgE selective unresponsiveness in a T-cell independent fashion. Cur Drug Targets Immune Endocr Metabol Disord 3: 119–135.
23. Nakano Y, Mori M, Yamamura H, Naito S, Kato H, et al. (2002) Cholesterol inclusion in liposomes affects induction of antigen-specific IgG and IgE antibody production in mice by a surface-coupled liposomal antigen. Bioconj Chem 13: 744–749.
24. Tanaka Y, Kasai M, Taneichi M, Naito S, Kato H, et al. (2004) Liposomes with differential lipid components exert differential adjuvanticity in antigen-liposome conjugates via differential recognition by macrophages. Bioconj Chem 15: 35–40.
25. Yewdell JW, Bennik JR (1999) Immunodominance in major histocompatibility complex class I-restricted T lymphocyte responses. Annu Rev Immunol 17: 51–88.
26. Yewdell JW, Haeryfar SM (2005) Understanding presentation of viral antigens to $CD8^+$ T cells in vivo: The key to rational vaccine design. Annu Rev Immunol 23: 651–682.
27. Watkins D (2008) The hope for an HIV vaccine based on induction of $CD8^+$ T lymphocytes. Mem Inst Oswaldo Cruz 103: 119–129.
28. Ishii S, Koziel MJ (2008) Immune responses during acute and chronic infection with hepatitis C virus. Clin Immunol 128: 133–147.
29. Zhu M (2004) SARS immunity and vaccination. Cell Mol Immunol 1: 193–198.
30. Guan Y, Poon LL, Cheung CY, Ellis TM, Lim W, et al. (2004) H5N1 influenza: A protean pandemic threat. Proc Natl Acad Sci 101: 8156–8161.
31. Webster RG, Govorkova EA (2006) H5N1 influenza - Continuing evolution and spread. N Engl J Med 355: 2174–2177.
32. Watanabe T, Watanabe S, Kim JH, Hatta M, Kawaoka Y (2008) Novel approach to the development of effective H5N1 influenza A virus vaccines: Use of M2 cytoplasmic tail mutants. J Virol 82: 2486–2492.
33. Skeik N, Jabr FI (2008) Influenza viruses and the evolution of avian influenza virus H5N1. Int J Infect Dis 12: 233–238.
34. Kreijtz JH, de Mutsert G, van Baalen CA, Fouchier RA, Osterhaus AD, et al. (2008) Cross-recognition of avian H5N1 influenza virus by human cytotoxic T-lymphocyte populations directed to human influenza A virus. J Virol 82: 5161–5166.
35. Heiny AT, Miotto O, Srinivasan KN, Khan AM, Zhang GL, et al. (2007) Evolutionarity conserved protein sequences of influenza a virus, avian and human, as vaccine targets. PLoS One 2: e1190.
36. Townsend ARM, Rothband J, Gotch FM, Bahadur G, Wraith D, et al. (1986) The epitopes of influenza nucleoprotein recognized by cytotoxic T lymphocytes can be defined with short synthetic peptides. Cell 44: 959–968.
37. Gotch F, McMichael A, Smith G, Moss B (1987) Identification of viral molecules recognized by influenza-specific human cytotoxic T lymphocytes. J Exp Med 165: 408–416.
38. Lee LY, Ann Ha DL, Simmons C, Jong MD, Chau NV, et al. (2008) Memory T cells established by seasonal human influenza A infection cross-react with avian influenza A (H5N1) in healthy individuals. J Clin Invest 118: 3478–3490.
39. Doherty PC, Kelso A (2008) Toward a broadly protective influenza vaccine. J Clin Invest 118: 3273–3275.
40. Epstein SL, Tumpey TM, Misplon JA, Lo CY, Cooper A, et al. (2002) DNA vaccin expressing conserved influenza virus proteins protective against H5N1 challenge infection in mice. Emerg Infect Dis 8: 796–801.
41. Nagata T, Toyota T, Ishigaki H, Ichihashi T, Kajino K, et al. (2007) Peptides coupled to the surface of a kind of liposome protect infection of influenza viruses. Vaccine 25: 4914–4921.
42. Matsui M, Kohyama S, Suda T, Yokoyama S, Mori M, et al. (2010) A CTL-based liposomal vaccine capable of inducing protection against heterosubtypic influenza viruses in HLA-A*0201 transgenic mice. Biochem Biophys Res Commun 391: 1494–1499.
43. Thomas PG, Keating R, Hulse-Post DJ, Doherty PC (2006) Cell-mediated protection in influenza infection. Emerg Infect Dis 12: 48–54.

OPEN ACCESS Freely available online

PLoS one

Liposome-Coupled Antigens Are Internalized by Antigen-Presenting Cells via Pinocytosis and Cross-Presented to CD8$^+$ T Cells

Yuriko Tanaka[1], Maiko Taneichi[2]*, Michiyuki Kasai[2], Terutaka Kakiuchi[1], Tetsuya Uchida[2]

1 Department of Immunology, Toho University School of Medicine, Tokyo, Japan, 2 Department of Safety Research on Blood and Biological Products, National Institute of Infectious Diseases, Tokyo, Japan

Abstract

We have previously demonstrated that antigens chemically coupled to the surface of liposomes consisting of unsaturated fatty acids were cross-presented by antigen-presenting cells (APCs) to CD8$^+$ T cells, and that this process resulted in the induction of antigen-specific cytotoxic T lymphocytes. In the present study, the mechanism by which the liposome-coupled antigens were cross-presented to CD8$^+$ T cells by APCs was investigated. Confocal laser scanning microscopic analysis demonstrated that antigens coupled to the surface of unsaturated-fatty-acid-based liposomes received processing at both MHC class I and class II compartments, while most of the antigens coupled to the surface of saturated-fatty-acid-based liposomes received processing at the class II compartment. In addition, flow cytometric analysis demonstrated that antigens coupled to the surface of unsaturated-fatty-acid-liposomes were taken up by APCs even in a 4°C environment; this was not true of saturated-fatty-acid-liposomes. When two kinds of inhibitors, dimethylamiloride (DMA) and cytochalasin B, which inhibit pinocytosis and phagocytosis by APCs, respectively, were added to the culture of APCs prior to the antigen pulse, DMA but not cytochalasin B significantly reduced uptake of liposome-coupled antigens. Further analysis of intracellular trafficking of liposomal antigens using confocal laser scanning microscopy revealed that a portion of liposome-coupled antigens taken up by APCs were delivered to the lysosome compartment. In agreement with the reduction of antigen uptake by APCs, antigen presentation by APCs was significantly inhibited by DMA, and resulted in the reduction of IFN-γ production by antigen-specific CD8$^+$ T cells. These results suggest that antigens coupled to the surface of liposomes consisting of unsaturated fatty acids might be pinocytosed by APCs, loaded onto the class I MHC processing pathway, and presented to CD8$^+$ T cells. Thus, these liposome-coupled antigens are expected to be applicable for the development of vaccines that induce cellular immunity.

Citation: Tanaka Y, Taneichi M, Kasai M, Kakiuchi T, Uchida T (2010) Liposome-Coupled Antigens Are Internalized by Antigen-Presenting Cells via Pinocytosis and Cross-Presented to CD8$^+$ T Cells. PLoS ONE 5(12): e15225. doi:10.1371/journal.pone.0015225

Editor: Derya Unutmaz, New York University, United States of America

Received August 3, 2010; **Accepted** November 1, 2010; **Published** December 17, 2010

Funding: This work was supported by grants from the Ministry of Health, Labor and Welfare of Japan (to TU), grants-in-aid for young scientists from the Japan Society for the Promotion of Science (21790963 to YT) and the research promotion grant from Toho University Graduate School of Medicine (No. 08-02 to YT). The funders had no role in study design, data collection and analysis, decision to publish, or preparation of the manuscript.

Competing Interests: The authors have declared that no competing interests exist.

* E-mail: taneichi@nih.go.jp

Introduction

Vaccines have played an important role in disease prevention and have made a substantial contribution to public health. Upon natural infection, it is known that the host responds by inducing both humoral and cellular immunity against the pathogen. However, most of the currently approved vaccines work by inducing humoral immunity [1–3]. For protection against viruses that are highly mutable and frequently escape from antibody-mediated immunity, such as influenza A viruses, HIV, and HCV, humoral immunity is insufficient [4–7]. Consequently, the development of vaccines that induce cellular immunity is critical to novel vaccine strategies.

T lymphocytes respond to peptide fragments of protein antigens that are displayed by MHC molecules on antigen-presenting cells (APCs). In general, extracellular antigens are presented via MHC class II molecules to CD4$^+$ T cells while intracellular antigens are presented via MHC class I molecules to CD8$^+$ T cells [8,9]. However, a number of reports have demonstrated that a significant level of crossover, so-called 'cross-presentation', occurs in APCs [10–14]. Using this phenomenon, novel vaccine preparation inducing antigen-specific CTLs that effectively eliminate virus-infected cells is expected. The mechanisms of cross-presentation have been studied intensively [15–17] while the details have been left unclear. Part of the antigens taken via phagocytosis by APCs are known to be translocated into the cytosol and degraded by local proteases [18,19]. In another pathway, some antigens internalized into endocytic compartments are loaded onto MHC class I molecules [20].

We previously reported that antigens chemically coupled to the surface of liposomes induced antigen-specific IgG but not IgE antibody production [21,22]. In addition, antigens chemically coupled to the surface of liposomes consisting of unsaturated fatty acids were presented not only to CD4$^+$- but also to CD8$^+$ T cells by APCs [23]. Since liposome-coupled antigens induce antiviral immunity [24,25], they are expected to be applicable for the development of viral vaccines without inducing antigen-specific IgEs, which cause allergic reactions. In the present study, we

investigated the mechanism by which the liposome-coupled antigens were cross-presented by APCs to $CD8^+$ T cells.

Results

Confocal laser scanning microscopic analysis of macrophages co-cultured with DQ-OVA-liposome conjugates

MHC class I of macrophages were stained with red fluorescein-labeled anti-mouse H-$2D^d$ mAb (Fig. 1A: left column), and MHC class II of macrophages were labeled with DM-DsRed (Fig. 1A: right column) as described in Materials and Methods. DQ-OVA, which exhibits green fluorescein upon proteolytic degradation, was coupled to liposomes consisting of unsaturated (oleoyl) or saturated (stearoyl) fatty acid, and added to the culture of macrophages. After incubation for 2 hr, the recovered macrophages were analyzed using confocal laser scanning microscopy. The results shown in Fig. 1 demonstrate that DQ-OVA coupled to oleoyl liposomes was processed at both MHC class I and class II compartments, while most of the DQ-OVA coupled to stearoyl liposomes was processed at the MHC class II compartment.

Differential manner of internalization by APCs of antigens coupled to liposomes with two kinds of lipid

$Alexa_{488}$-labeled OVA were coupled to liposomes and were added to the cultures of macrophages. As shown in Fig. 2, OVA coupled to oleoyl liposomes were internalized by APCs more efficiently than those coupled to stearoyl liposomes at 37°C. Interestingly, OVA coupled to oleoyl liposomes but not stearoyl liposomes were internalized significantly by APCs even in a 4°C environment.

Effect of inhibitors on uptake of liposome-coupled antigens by APCs

One of two kinds of inhibitors, cytochalasin B and DMA, which inhibit APC phagocytosis and pinocytosis of antigens, respectively, was added to the culture of macrophages 1 hr prior to the addition of $Alexa_{488}$-OVA- or DQ-OVA-coupled oleoyl liposomes. One hour later, flow cytometric analysis was performed. As shown in Fig. 3, the effect of cytochalasin B on the antigen uptake and digestion of liposome-coupled OVA by APCs was limited. On the other hand, DMA significantly reduced both antigen uptake and digestion of antigens by macrophages.

Localization of antigens coupled to liposomes in APCs

DQ-OVA-coupled oleoyl liposomes were added to the culture of macrophages in which either EEA1 or LAMP-1 were co-stained. The co-localization of the liposome-coupled antigens and intracellular organelles in the APCs was analyzed using confocal laser scanning microscopy. As shown in Figure 4, although most of the DQ-OVA coupled to oleoyl liposomes was processed beyond LAMP-1-expressing compartments (green spots), a portion of DQ-OVA was processed at compartments expressing LAMP-1 (yellow spots). Co-localization of EEA1-expressing compartments with liposome-coupled-DQ-OVA was significantly less than that of LAMP-1-expressing compartments with DQ-OVA (Fig. 4B).

T cell activation by APCs pulsed with liposomal antigen

In agreement with the results shown in Fig. 3, antigen presentation by APCs pulsed with liposomal antigen was significantly inhibited by DMA but not by cytochalasin B in both $CD4^+$- and $CD8^+$ T cell responses (Fig. 5).

Discussion

In general, extracellular antigens are presented via MHC class II molecules to $CD4^+$ T cells, whereas intracellular antigens are presented via MHC class I molecules to $CD8^+$ T cells. Consequently, most APCs do not present exogenous antigens via MHC class I since exogenous antigens do not gain access to the cytosolic compartment. Therefore, exogenous antigens usually do not prime CTL responses *in vivo*. This segregation of exogenous antigens from the class I pathway is important to prevent CTL from killing healthy cells that have been exposed to foreign antigens but are not infected [26]. However, there are several exceptions to this rule, reflecting the ability of the exogenous antigens to be delivered into the cytosolic compartments [13–17].

We have previously reported that antigens coupled to the surface of liposomes comprised of unsaturated fatty acid are presented to both $CD4^+$- and $CD8^+$ T cells [23]. Confocal laser scanning microscopic analysis demonstrated that a portion of the liposome-coupled antigens were taken up and processed beyond the MHC class II compartment. In the present study, we confirmed that OVA coupled to oleoyl liposomes was processed at both the MHC class I and class II compartments (Fig. 1). Flow cytometric analysis demonstrated that OVA coupled to oleoyl liposomes was incorporated more efficiently by macrophages than OVA coupled to stearoyl liposomes (Fig. 2). Furthermore, OVA coupled to oleoyl liposomes was taken up by macrophages even in a 4°C environment, in which antigen entry could only occur via plasma membrane translocation. In general, antigen processing pathways largely depend on the route of antigen uptake, and liposomes with a certain lipid component are known to fuse with the plasma membrane [27]. The uptake of OVA coupled to oleoyl liposomes in a 4°C environment observed in the present study suggested that oleoyl liposome might fuse with the plasma membrane and thereby allow the liposome-coupled antigen direct access to the cytosol. The role of endocytosis in the uptake of the liposomal antigen was further examined by using specific inhibitors for antigen uptake (Fig. 3). Cytochalasin B treatment of APCs prior to the addition of liposomal antigen in the culture had little effect. However, treatment of APCs with DMA significantly reduced the uptake of liposome-coupled OVA. Consequently, it was suggested that antigens coupled to oleoyl liposomes might be taken up by APCs via at least two pathways, penetration and pinocytosis. The analysis of intracellular pathways of antigens coupled to oleoyl liposomes using confocal laser scanning microscopy demonstrated that a portion of liposomal antigens taken up by APC were translocated to the lysosomal compartments expressing LAMP-1 (Fig. 4), suggesting that the liposomal antigens processed at lysosomal compartment and beyond lysosomal compartment might be presented to CD4/$CD8^+$ T cells via MHC class II and class I, respectively. In agreement with the results of antigen uptake shown in Fig. 3, the treatment of splenic $CD11c^+$ cells with DMA significantly reduced antigen presentation of liposomal antigens to both $CD4^+$- and $CD8^+$ T cells as evaluated by T-cell activation (Fig. 5).

It was reported that pinocytosis and scavenger receptor-mediated endocytosis by APC facilitate antigen presentation to $CD4^+$ T cells; by contrast, mannose receptor-mediated endocytosis by APC has been shown to facilitate antigen presentation to $CD8^+$ T cells [28]. However, as described in Materials and Methods, the oleoyl liposomes used in the present study do not contain mannose.

Thus, the data in the present study demonstrated that antigens coupled to oleoyl liposomes were internalized by APCs through both penetration and pinocytosis. The antigens coupled to the surface of oleoyl liposomes were processed at both MHC class I

A

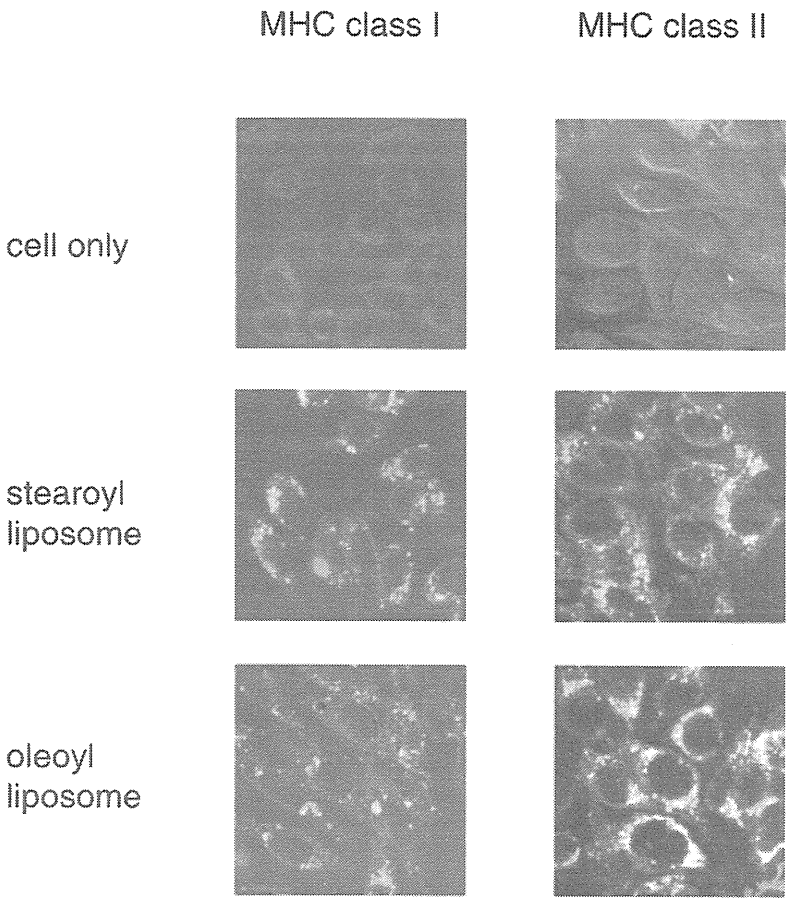
MHC class I
MHC class II
cell only
stearoyl liposome
oleoyl liposome

B

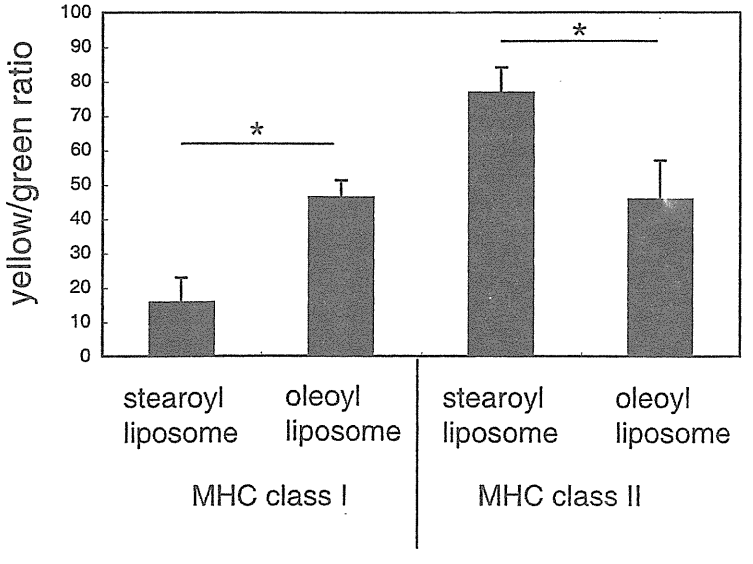
yellow/green ratio
100
90
80
70
60
50
40
30
20
10
0
*
*
stearoyl liposome
oleoyl liposome
stearoyl liposome
oleoyl liposome
MHC class I
MHC class II

Figure 1. Confocal laser scanning microscopic analysis of macrophages co-cultured with DQ-OVA-liposome conjugates. A, DQ-OVA was coupled to either stearoyl or oleoyl liposomes and added to the culture of cloned macrophages expressing DM-DsRed (class II) or labeled with red fluorescein (class I), as described in Materials and Methods. Two hours after the onset of the culture, macrophages were recovered and analyzed using confocal laser scanning microscopy. These optically merged images are representative of most cells examined by confocal microscopy. Yellow, co-localization of green (DQ-OVA after proteolytic degradation) and red (macrophage DM or class I); cell only, macrophages without co-culture with DQ-OVA-coupled liposomes. B, the green- and yellow-color compartments in the immunofluorescent pictures were quantified by the image analysis software MetaMorph, as described in Materials and Methods. Ratios of the yellow to green compartments are shown. Data represent the mean values ± SD of the images shown in Fig. 1A. Asterisk, significant ($p<0.01$) difference of samples.
doi:10.1371/journal.pone.0015225.g001

and class II compartments and presented to $CD4^+$- and $CD8^+$ T cells. Although the detailed pathway leading to presentation to both $CD4^+$- and $CD8^+$ T cells remains unclear, the observed behavior of antigens coupled to oleoyl liposome in APCs seems quite unique. Taken together, coupling of antigens to oleoyl liposome might potentially serve as a novel method to induce both humoral and cellular immunity.

Materials and Methods

Mice

CBF1 mice (8 weeks of age, female) were purchased from SLC (Shizuoka, Japan). All experiments were approved (No. 208021 and 209082) by an independent animal ethics committee at National Institute of Infectious Diseases, Tokyo, Japan.

Chemicals

All phospholipids were provided by NOF Co. (Tokyo, Japan). Reagent grades of cholesterol were purchased from Wako Pure Chemical (Osaka, Japan).

Antigens and reagents

Ovalbumin (OVA, Grade VII) was purchased from Sigma-Aldrich. For the analysis of the processing of liposome-coupled OVA by macrophages, DQ-OVA, which exhibits green fluores-

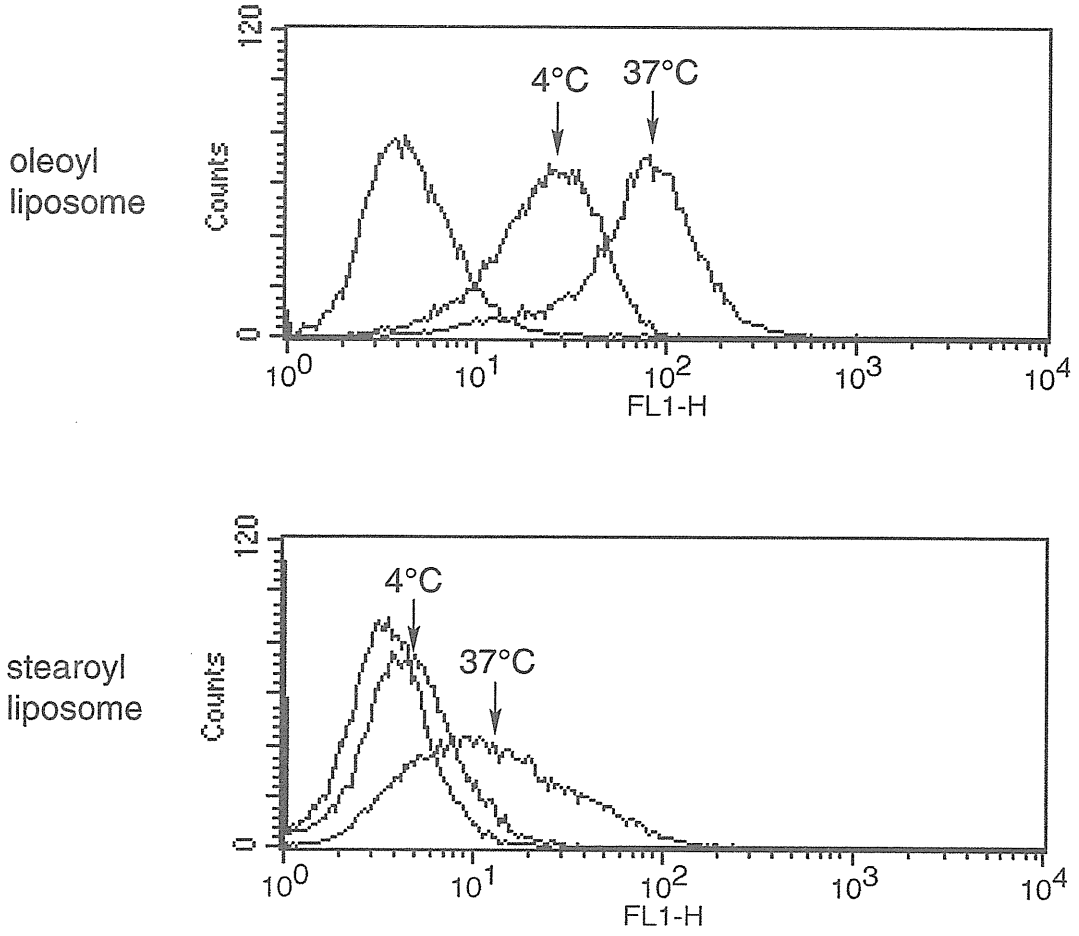

Figure 2. Uptake of liposome-coupled OVA by macrophages. Alexa-labeled OVA was coupled to either stearoyl or oleoyl liposomes and added to the culture of cloned macrophages as described in Materials and Methods. Thirty minutes after the onset of the culture, macrophages were recovered and analyzed using flow cytometry.
doi:10.1371/journal.pone.0015225.g002

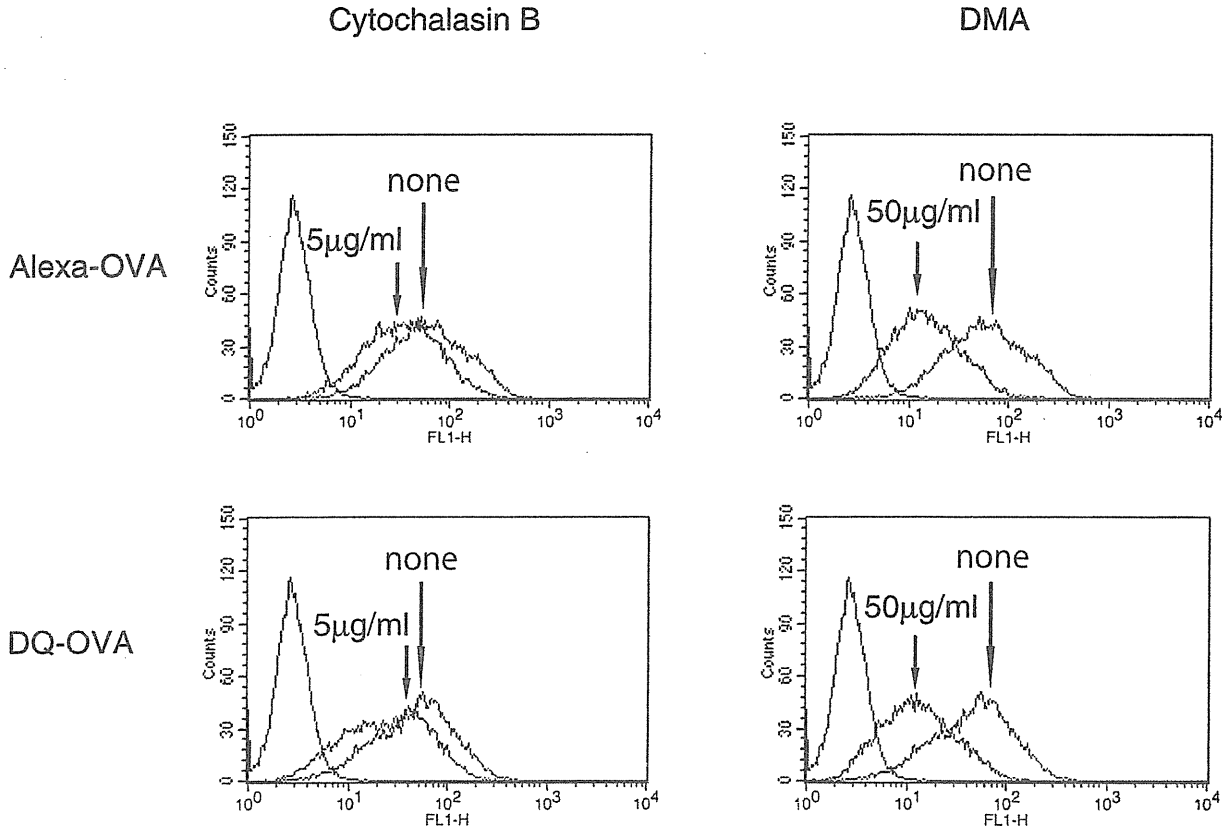

Figure 3. Influence of inhibitors for uptake of OVA coupled to oleoyl liposomes by macrophages. Alexa- or DQ-labeled OVA was coupled to oleoyl liposomes and added to the culture of macrophages as described in Materials and Methods. Treatment of macrophages with cytochalasin B or DMA was done 60 minutes prior to the addition of OVA-liposome conjugates.
doi:10.1371/journal.pone.0015225.g003

cence upon proteolytic degradation, was purchased from Molecular Probes, Inc. Synthetic CpG ODN (5002: TCCATGACGTTCTTGATGTT) was purchased from Invitrogen and was phosphorothioate-protected to avoid nuclease-dependent degradation.

Fluorescence labeling of OVA

OVA was labeled with fluorescence using an AlexaFluor 488 protein labeling kit (Invitrogen) according to the manufacturer's protocol.

Liposomes

Liposomes consisting of two different kinds of lipid were used in this study. Liposomes consisting of saturated fatty acids were composed of distearoyl phosphatidylcholine, distearoyl phosphatidyl ethanolamine, distearoyl phosphatidyl glycerol acid, and cholesterol in a 4:3:2:7 molar ratio (stearoyl liposomes), and liposomes consisting of unsaturated fatty acids were composed of dioleoyl phosphatidylcholine, dioleoyl phosphatidyl ethanolamine, dioleoyl phosphatidyl glycerol acid, and cholesterol in a 4:3:2:7 molar ratio (oleoyl liposomes). The crude liposome solution was passed through a membrane filter (nucleopore polycarbonate filter, Coster) with a pore size of 0.2 mm.

Coupling of OVA to liposomes

Liposomal conjugates with plain OVA, Alexa-labeled OVA, or DQ-OVA were prepared essentially in the same way as described previously [22]. Briefly, to a mixture of 90 mg of liposomes and 6 mg of OVA in 2.5 ml phosphate buffer (pH 7.2), 0.5 ml of 2.5% glutaraldehyde solution was added in dropwise fashion. The mixture was stirred gently for 1 h at 37°C, and then 0.5 ml of 3 M glycine-NaOH (pH 7.2) was added to block excess aldehyde groups. This was followed by incubation overnight at 4°C. The liposome-coupled OVA and uncoupled OVA in the resulting solution were separated using CL-4B column chromatography (Pharmacia). The amount of lipid in the liposomal fraction was measured using a phospholipid content assay kit (Wako Pure Chemical). The OVA-liposome solution was adjusted to 10 mg lipid/ml in PBS, sterile-filtered using a Millex-HA syringe filter unit (0.45 μm, Millipore), and kept at 4°C until use.

Quantification of OVA coupled to liposome

For the measurement of OVA coupled to liposome, radiolabeled OVA (*methyl*-^{14}C; purchased from New England Nuclear) was mixed with cold OVA and used for coupling with liposome and for determining the calibration curve. The

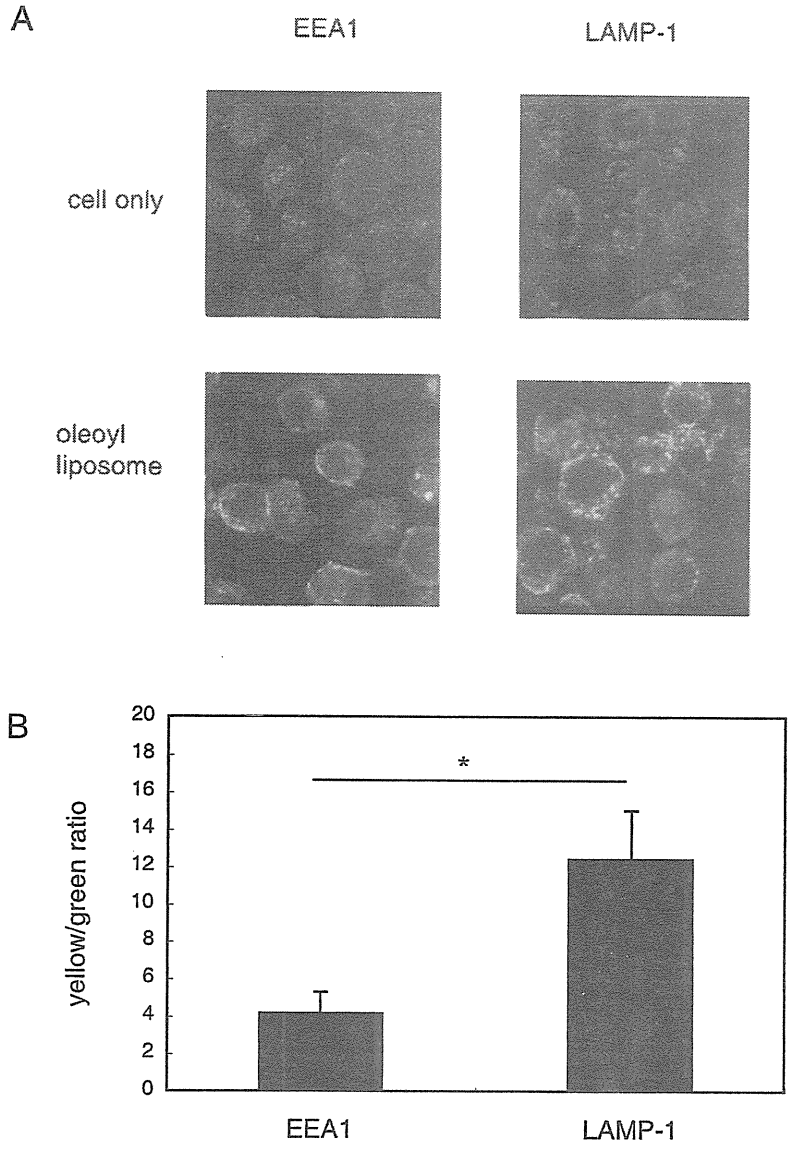

Figure 4. Intracellular localization of liposomal antigens taken up by macrophages. A, DQ-OVA was coupled to oleoyl liposomes and added to the culture of cloned macrophages of which endosomal marker EEA1-positive compartments, or lysosomal marker LAMP-1-positive compartments were stained as described in Materials and Methods. Two hours after the onset of the culture, macrophages were recovered and analyzed using confocal laser scanning microscopy. These optically merged images are representative of most cells examined by confocal microscopy. Yellow, co-localization of green (DQ-OVA after proteolytic degradation) and red (macrophage EEA1 or LAMP-1); cell only, macrophages without co-culture with DQ-OVA liposomes. B, the green- and yellow-color compartments in the immunofluorescent pictures were quantified by the image analysis software MetaMorph, as described in Materials and Methods. Ratios of the yellow to green compartments are shown. Data represent the mean values ± SD of the images shown in Fig, 4A. Asterisk, significant ($p<0.01$) difference of samples.
doi:10.1371/journal.pone.0015225.g004

radioactivity of the resulting OVA-liposome solution was counted using a calibration curve. The amounts of OVA coupled to stearoyl and oleoyl liposomes were 47.0 and 46.8 μg/mg lipid, respectively.

Immunization

Mice were immunized subcutaneously (s.c.) with the OVA-liposome conjugate at a dose of 1 mg lipid/100 μl/mouse in the presence of 5 μg/mouse CpG.

Cloned macrophage hybridoma

Macrophage hybridoma clone 39, obtained from the fusion of splenic adherent cells from CKB mice and P388D1 [29], was used.

Construction and expression of the fusion protein, DM-DsRed, in macrophage clone 39

The DNA fragment coding the full-length H2-DMβ2 [30] was amplified by PCR with two primers (5′-ATGGCTGCACT-CTGGCTGCTGCTGCTGGT-3′ and 5′-GATGCCGTCCT-

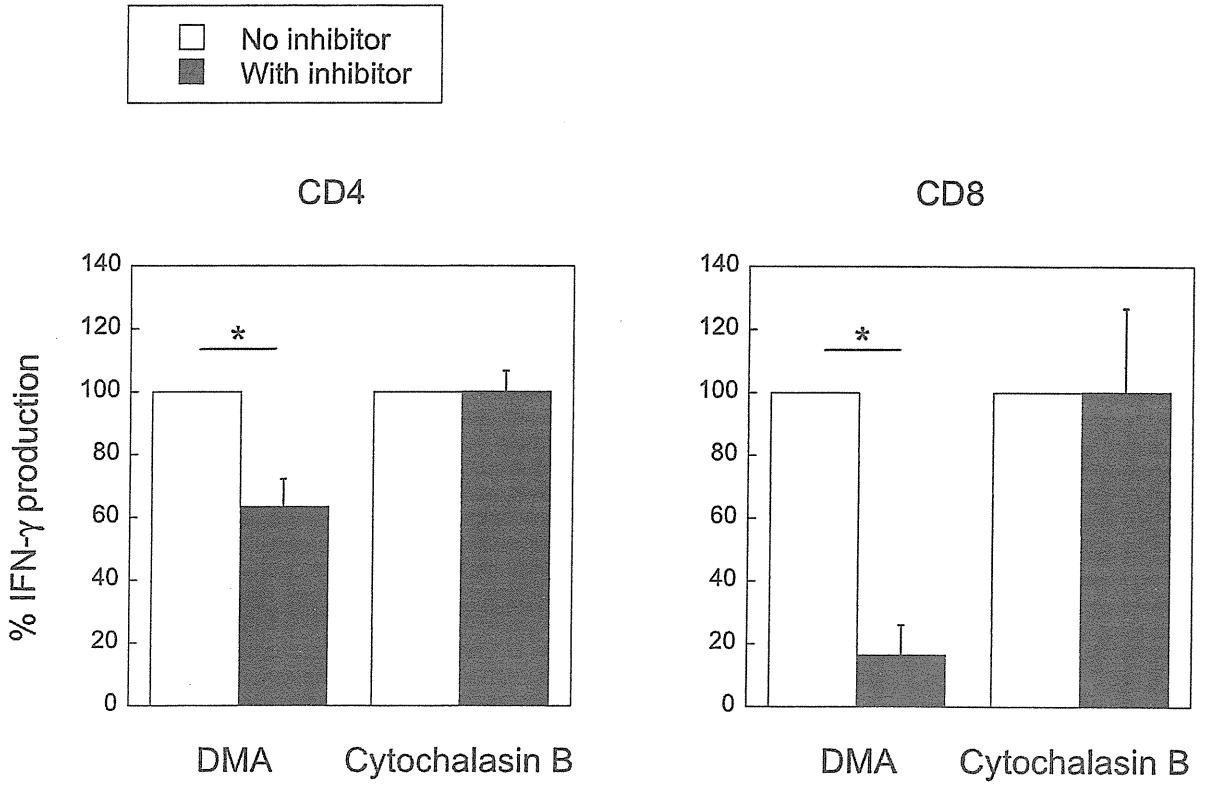

Figure 5. IFN-γ production by splenic CD4/CD8$^+$ T cells of mice immunized with OVA after co-culture with CD11c$^+$ cells pulsed with OVA coupled to oleoyl liposomes. Splenic CD4/CD8$^+$ T cells were taken from mice immunized with OVA and were cultured with CD11c$^+$ cells pulsed with OVA coupled to oleoyl liposomes with or without inhibitors as described in Materials and Methods. IFN-γ production of T cells in the supernatants in the absence of inhibitors was normalized to 100%. Data represent the mean values ± SD of triplicate culture. Asterisk, significant ($p<0.01$) difference as compared with the 'no inhibitor' group.
doi:10.1371/journal.pone.0015225.g005

TCTGGGTAGGTGGATCC-3′). The PCR product was cloned into the CMV promoter-driven expression plasmid pDsRedN1 (BD Clontech). This construct omitted the stop codon of H2-DMβ2 and encoded the H2-DMβ2 fused with DsRed. The cloned plasmid DNA was transfected to macrophage hybridoma clone 39 with Effectene transfection reagent (Qiagen) according to the manufacturer's protocol. During the transfection to clone 39, the medium containing cDNA and the transfection reagent was replaced with fresh medium after an 8-h transfection, and then clone 39 was cultured for 40 h. To obtain stable cell lines, clone 39 was passaged at 1:5 into RPMI 1640 containing 10% FCS with 50 μg/ml geneticin (G-418; Sigma-Aldrich). Cells showing the best fluorescence were selected using a FACS Vantage cell sorter (BD Bioscience). After cell sorting, clone 39 expressing DM-DsRed was cultured in RPMI 1640 containing 10% FCS with 200 μg/ml geneticin.

Flow cytometry

To investigate the capture of OVA-liposome conjugates by macrophages, macrophage clone 39 was incubated for 30 min at 4°C or 37°C in the presence of fluorescence-labeled OVA-liposome conjugates that contained a final concentration of 4 μg/ml OVA. After the incubation, cells were washed with ice-cold PBS. In the case of using Alexa-labeled OVA-liposome conjugates, cells were then incubated with 1.2 μg/ml trypan-blue for 5 min at 4°C to block the fluorescence of Alexa-OVA attached to the cell surface. After the cells were washed, they were analyzed on a FACS Caliber flow cytometer (BD Bioscience). The histograms of fluorescence distribution were plotted as the number of cells versus fluorescence intensity on a logarithmic scale.

Confocal laser scanning microscopy

To investigate the localization of OVA-liposome conjugates by macrophages, macrophage clone 39 or DM-DsRed-expressing cloned macrophage 39 was cultured for 18 h at 37°C on 8-hole heavy Teflon-coated slides (Bokusui Brown) and was then incubated with DQ-OVA-liposome conjugates, prepared using oleoyl or stearoyl liposomes, for 2 h at 37°C. The slides were then washed with MEM and fixed with 4% paraformaldehyde in PBS for 10 min at room temperature. After fixation, they were incubated for 10 min in 0.1 M glycine-HCl (pH 7.0) to block the remaining aldehyde residue. They were then washed two times in PBS. After washing, the slides were sealed with PBS:glycerin (1:9) and analyzed under an LSM510 confocal laser scanning microscope system (Zeiss). For analysis of co-localization of OVA and MHC class I, early endosomal antigen 1 (EEA1) or lysosomal-associated membrane protein-1 (LAMP-1) after blocking of the remaining aldehyde residue, cloned macrophage 39 was subsequently permeabilized with 0.05% saponin-TBS for 10 min at room temperature. After being washed twice with PBS, they were reacted with biotin-conjugated mouse anti-mouse H-2D^d mAb (34-2-12, 10 μg/ml; BD Biosciences), goat anti-mouse EEA1

polyclonal antibody (N19, 1 μg/ml; Santa Cruz Biotechnology) or rat anti-mouse LAMP-1 monoclonal antibody (1D4B, 1 μg/ml; Santa Cruz Biotechnology) for 18 h at 4°C. After being washed three times with TBS, they were reacted with Alexa 546-conjugated streptavidin (1:200 diluted; Invitorogen) to detect MHC class I, Alexa Fluor 568-labeled Ab (rabbit anti-goat IgG, 10 μg/ml; Invitrogen) to detect EEA1 or Alexa Fluor 568-labeled Ab (goat anti-rat IgG, 10 μg/ml; Invitrogen) to detect LAMP-1 for 4 h at room temperature. They were then washed two times in TBS. After the washing, the slides were sealed with PBS:glycerin (1:9) and analyzed under an LSM510 confocal laser scanning microscope system (Zeiss).

Quantification of immunofluorescent pictures and statistics

Quantification of confocal image analysis was done by single cell identification using the image analysis software MetaMorph (Molecular Devices Co., Tokyo, Japan), and the relative fluorescence intensity of green, red, and yellow pixels was assessed. The relative fluorescence intensity of all individual colors was then expressed as percent of the total fluorescence intensity. p values were calculated by the Student's t test with two-tailed distribution and two-sample unequal variance parameters.

Inhibition Studies of Antigen Uptake

In the case of inhibition studies, cloned macrophage 39 or $CD11c^+$ cells were incubated with indicated inhibitors 60 min before and throughout the antigen pulse. Cytochalasin B [31] and DMA [28] were purchased from Sigma.

Preparation of $CD11c^+$ cells and $CD4^+$- and $CD8^+$ T cells

$CD11c^+$ spleen cells of naïve mice and $CD4^+$ T and $CD8^+$ T spleen cells of mice immunized with OVA-liposome conjugates were prepared with the magnetic cell sorter system MACS, according to the manufacturer's protocol using anti-CD11c, anti-CD4 and anti-CD8 antibody-coated microbeads (Miltenyi Biotec).

Culture of $CD4^+$- and $CD8^+$ T cells with $CD11c^+$ cells pulsed with OVA

$CD11c^+$ cells were incubated with or without the indicated inhibitors for 60 min in a 24-well plate prior to the addition of OVA-liposome conjugates made using oleoyl liposomes. The final concentration of OVA-liposome added to the macrophage culture was 500 μg lipid/ml, which included 24 μg OVA. After 60 minutes' incubation, $CD11c^+$ cells were washed 3 times in ice-cold medium and 2×10^5 cells were co-cultured with 5×10^5 $CD4^+$ T cells or $CD8^+$ T cells, in a 48-well plate. A preliminary experiment showed that the optimal culture period in the above culture condition was 2 days for IFN-γ production by $CD4^+$ T cells and 5 days for IFN-γ production by $CD8^+$ T cells. After incubation in a CO_2 incubator for 2 or 5 days, the culture supernatants were collected and assayed for IFN-γ.

IFN-γ Assay

IFN-γ in the culture supernatants was measured using the Biotrak mouse ELISA system (GE Healthcare). All test samples were assayed in duplicate, and the SD in each test was always <5% of the mean value.

Author Contributions

Conceived and designed the experiments: MT TU. Performed the experiments: YT MT TK TU. Analyzed the data: MT MK TU. Contributed reagents/materials/analysis tools: MT TU. Wrote the paper: MT TU.

References

1. Mark A, Björkstén B, Granstörm M (1995) Immunoglobulin E responses to diphtheria and tetanus toxoids after booster with aluminium-adsorbed and fluid DT-vaccines. Vaccine 13: 669–673.
2. Aggerbeck H, Wantzin J, Heron I (1996) Booster vaccination against diphtheria and tetanus in man. Comparison of three different vaccine formulations – III. Vaccine 14: 1265–1272.
3. Nothdurft HD, Jelinek T, Marschang A, Maiwald H, Kapaun A, et al. (1996) Adverse reactions to Japanese encephalitis vaccine in travelers. J Infect 32: 119–122.
4. Doherty PC, Kelso A (2008) Toward a broadly protective influenza vaccine. J Clin. Invest 118: 3273–3275.
5. McMichael AJ, Hanke T (2003) HIV vaccines 1983-2003. Nat. Med 9: 874–880.
6. Chen M, Sallberg M, Sonnerberg A, Weiland L, Mattsson L, et al. (1999) Limited humoral immunity in hepatitis C virus infection. Gastroenterology 116: 135–143.
7. Yerly D, Heckerman D, Allen TM, Chsiholm JV, III, Faircloth K, et al. (2008) Increased cytotoxic T-lymphocyte epitope variant cross-recognition and functional avidity are associated with hepatitis C virus clearance. J Virol 82: 3147–3153.
8. Bevan MJ (1987) Antigen recognition. Class discrimination in the world of immunology. Nature 325: 192–194.
9. Germain RN, Margulies DH (1993) The biochemistry and cell biology of antigen processing and presentation. Annu Rev Immunol 11: 403–450.
10. Norbury CC, Hewlett LJ, Prescott AR, Shastri N, Watts C (1995) Class I MHC presentation of exogenous soluble antigen via macropinocytosis in bone marrow macrophages. Immunity 3: 783–791.
11. Nelson D, Bundell C, Robinson B (2000) In Vivo Cross-presentation of a soluble protein antigen: kinetics, distribution, and generation of effect CTL recognizing dominant and subdominant epitopes. J Immunol 165: 6123–6132.
12. Chen W, Masterman K-A, Basta S, Haeryfer SMM, Dimopoulos N, et al. (2004) Cross-priming of $CD8^+$ T cells by viral and tumor antigens is a robust phenomenon. Eur J Immunol 34: 194–199.
13. Bevan MJ (1976) Cross-priming for a secondary cytotoxic response to minor H antigens with *H-2* congenic cells which do not cross-react in the cytotoxic assay. J Exp Med 143: 1283–1288.
14. Bevan MJ (2006) Cross-priming, Nat Immunol 7: 363–365.
15. Vyas JM, Veen AGVD, Ploegh HL (2008) The known unknown of antigen processing and presentation, Nature Rev Immunol 8: 607–618.
16. Kasturi SP, Pulendran B (2008) Cross-presentation: avoiding trafficking chaos? Nat Immunol 9: 461–463.
17. Rock KL (2003) The ins and outs of cross-presentation. Nat Immunol 4: 941–943.
18. Bankowski MK, Rock KL (1995) A phagosome-to-cytosol pathway for exogenous antigens presented on MHC class I molecules. Science 267: 243–246.
19. Rodriguez A, Regnault A, Kleijmeer M, Ricciardi-Castagnoli P, Amigorena S (1999) Selective transport of internalized antigens to cytosol for MHC class I presentation in dendritic cells. Nat Cell Biol 1: 362–368.
20. Shen L, Sigal LJ, Boes M, Rock KL (2004) Important role of cathepsin S in generating peptides for TAP-independent MHC class I crosspresentation in vivo. Immunity 21: 155–165.
21. Naito S, Horino A, Nakayama M, Nakano Y, Nagai T, et al. (1996) Ovalbumin-liposome conjugate induces IgG but not IgE antibody production. Int Arch Allergy Immunol 109: 223–228.
22. Nakano Y, Mori M, Nishinohara S, Takita Y, Naito S, et al. (1999) Antigen-specific, IgE-selective unresponsiveness induced by antigen-liposome conjugates. Comparison of four different conjugation methods for the couplong of antigen to liposome. Int Arch Allergy Immunol 120: 199–208.
23. Taneichi M, Ishida H, Kajino K, Ogasawara K, Tanaka Y, et al. (2006) Antigen chemically coupled to the surface of liposomes are cross-presented to $CD8^+$ T cells and induce potent antitumor immunity. J Immunol 177: 2324–2330.
24. Ohno S, Kohyama S, Taneichi M, Moriya O, Hayashi H, et al. (2009) Synthetic peptides coupled to the surface of liposomes effectively induce SARS coronavirus-specific cytotoxic T lymphocytes and viral clearance in HLA-A*0201 transgenic mice, Vaccine 27: 3912–3920.
25. Matsui M, Kohyama S, Suda S, Yokoyama S, Mori M, et al. (2010) A CTL-based liposomal vaccine capable of inducing protection against heterosubtypic influenza viruses in HLA-A*0201 transgenic mice. Biochem Biophys Res Commun 391: 1494–1499.
26. Rock KL (2006) Exiting the outside world for cross-presentation. Immunity 25: 523–525.
27. Felgner PL, Gadek TR, Holm M, Roman R, Chan HW, et al. (1987) Lipofection: a highly efficient, lipid-mediated DNA-transfection procedure. Proc. Natl Acad Sci USA 84: 7413–7417.

28. Burgdorf S, Kautz A, Böhnert V, Knolle PA, Kurts C (2007) Distinct pathways of antigen uptake and intracellular routing in CD4 and CD8 T cell activation. Science 316: 612–616.
29. Uchida T, Ju S, Fay A, Liu Y, Dorf ME (1985) Functional analysis of macrophage hybridomas. I. Production and initial characterization. J Immunol 134: 772–778.
30. Hermel E, Yuan J, Monaco JJ (1995) Characterization of polymorphism within the H2-M MHC class II loci. Immunogenetics 42: 136–142.
31. Gurnani K, Kennedy J, Sad S, Sprott GD, Krishnan L (2004) Phosphatidylserine receptor-mediated recognition of archaeosome adjuvant promotes endocytosis and MHC class I cross-presentation of the entrapped antigen by phagosome-to-cytosol transport and classical processing. J Immunol 173: 566–578.

Journal of Virological Methods 171 (2011) 310–313

Contents lists available at ScienceDirect

Journal of Virological Methods

journal homepage: www.elsevier.com/locate/jviromet

Short communication

Detection of all known filovirus species by reverse transcription-polymerase chain reaction using a primer set specific for the viral nucleoprotein gene

Hirohito Ogawa[a,b], Hiroko Miyamoto[b], Hideki Ebihara[c], Kimihito Ito[b], Shigeru Morikawa[d], Heinz Feldmann[c], Ayato Takada[b,*]

[a] Hokudai Center for Zoonosis Control in Zambia, School of Veterinary Medicine, The University of Zambia, P.O. Box 32379, Lusaka, Zambia
[b] Hokkaido University Research Center for Zoonosis Control, Kita-20, Nishi-10, Kita-ku, Sapporo 001-0020, Japan
[c] Laboratory of Virology, Division of Intramural Research, National Institute of Allergy and Infectious Diseases, National Institutes of Health, Rocky Mountain Laboratories, Hamilton, MT, USA
[d] Department of Virology 1, National Institute of Infectious Diseases, 4-7-1 Gakuen, Musashimurayama, Tokyo 208-0011, Japan

Article history:
Received 7 July 2010
Received in revised form 5 November 2010
Accepted 10 November 2010
Available online 17 November 2010

Keywords:
Filovirus
Marburg virus
Ebola virus
Diagnosis
RT-PCR

A B S T R A C T

The filoviruses, Marburg virus (MARV) and Ebola virus (EBOV), are causative agents of severe hemorrhagic fever with high mortality rates in humans and non-human primates. Sporadic outbreaks of filovirus infection have occurred in Central Africa and parts of Asia. Identification of the natural reservoir animals that are unknown yet and epidemiological investigations are current challenges to forestall outbreaks of filovirus diseases. The filovirus species identified currently include one in the MARV group and five in the EBOV group, with large genetic variations found among the species. Therefore, it has been difficult to develop a single sensitive assay to detect all filovirus species, which would advance laboratory diagnosis greatly in endemic areas. In this study, a highly sensitive universal RT-PCR assay targeting the nucleoprotein (NP) gene of filoviruses was developed. The genomic RNAs of all known MARV and EBOV species were detected by using an NP-specific primer set. In addition, this RT-PCR procedure was verified further for its application to detect viral RNAs in tissue samples of animals infected experimentally and blood specimens of infected patients. This assay will be a useful method for diagnostics and epidemiological studies of filovirus infections.

Marburg virus (MARV) and Ebola virus (EBOV) are enveloped, single-stranded, negative-sense RNA viruses classified into two genera, *Marburgvirus* and *Ebolavirus*, in the family *Filoviridae*, order *Mononegavirales* (Feldmann et al., 2004). These viruses are causative agents of severe hemorrhagic fever with high mortality rates in humans and non-human primates (Feldmann et al., 2003). There is a single *Marburgvirus* species, *Lake Victoria marburgvirus* (LVMARV), whereas there are four known *Ebolavirus* species, *Zaire ebolavirus* (ZEBOV), *Sudan ebolavirus* (SEBOV), *Reston ebolavirus* (REBOV) and *Cote d'Ivoire ebolavirus* (CIEBOV) (Feldmann et al., 2004). The genomic structures of filoviruses are very similar and approximately 19 kilobases in length, containing seven genes arranged sequentially in the order nucleoprotein (NP)-viral protein (VP) 35-VP40-glycoprotein-VP30-VP24-RNA polymerase (L) (Sanchez et al., 2006).

Since the discovery of Marburg hemorrhagic fever in Germany in 1967, sporadic outbreaks of Marburg and Ebola hemorrhagic fever have been reported from different countries in Central Africa (Feldmann et al., 2003). Incidences have increased in Central Africa since the beginning of the new millennium (Centers for Disease Control and Prevention, 2010a, b), and *Bundibugyo ebolavirus* (BEBOV) which has been proposed as a fifth species of EBOV was discovered recently in Uganda (Towner et al., 2008). Furthermore, two imported cases of Marburg hemorrhagic fever (in the Netherlands and the United States) (Centers for Disease Control and Prevention, 2009; Timen et al., 2009) and one of Ebola hemorrhagic fever (in South Africa) (World Health Organization, 1997) in travelers, have been reported, emphasizing the risk of filovirus infection in non-endemic countries.

Real-time RT-PCR (Drosten et al., 2002; Gibb et al., 2001; Weidmann et al., 2004) and reverse transcription-loop-mediated isothermal amplification (RT-LAMP) methods (Kurosaki et al., 2007, 2010) have been published recently for the diagnosis of filovirus infections. However, the real-time RT-PCR requires expensive, sophisticated equipment and thus does not seem to be practical for routine use in endemic areas such as Africa, and false-positive reactions in RT-LAMP cannot be discriminated since it does not

* Corresponding author at: Department of Global Epidemiology, Hokkaido University Research Center for Zoonosis Control, Kita-20, Nishi-10, Kita-ku, Sapporo 001-0020, Japan. Tel.: +81 11 706 9502; fax: +81 11 706 7310.
E-mail address: atakada@czc.hokudai.ac.jp (A. Takada).

0166-0934/$ – see front matter © 2010 Elsevier B.V. All rights reserved.
doi:10.1016/j.jviromet.2010.11.010

provide valuable nucleotide sequence information on its products. More importantly, these methods established previously are relatively species-specific and cannot be applied reliably in diagnostics and field studies for the broad detection of filoviruses, including potential new species. For example, this was the case for BEBOV infections, which were not detected initially by using real-time RT-PCR specific for the filoviruses species known previously, ZEBOV, SEBOV, and MARV (Towner et al., 2008). In fact, only one sample out of 20 human blood specimens suspected was positive in conventional RT-PCR using the currently available universal filovirus primers, FILO-A and FILO-B (Sanchez et al., 1999; Towner et al., 2008). Therefore, it is important to design new primers for RT-PCR allowing the broad detection of filovirus genomic RNA. In this study, nucleotide sequences of all known filovirus species were compared and a new assay for the detection of all known filoviruses using a primer set targeting a highly conserved region in the NP gene was evaluated.

One-step RT-PCR was carried out using a QIAGEN OneStep RT-PCR Kit (QIAGEN GmbH, Hilden, Germany) according to the manufacturer's instructions. A total volume of 25 μl of reaction mixture containing 0.2 μM of each primer and 1 μl of template RNA was used. Four primers targeting MARV and EBOV NP genes (FiloNP primers) were designed (Table 1). The one-step RT-PCR program consisted of reverse transcription at 50 °C for 30 min, initial PCR activation at 95 °C for 15 min, followed by 50 cycles of denaturation at 94 °C for 15 s, annealing at 53 °C for 30 s, extension at 72 °C for 30 s, and final extension at 72 °C for 7 min (Veriti 200 thermal cycler; Life Technologies Co., Carlsbad, CA). For comparison, the primers published previously, FILO-A and FILO-B, were used under the same conditions.

LVMARV (Popp, Ozolin, Musoke, Ravn, and Angola #368), ZEBOV (Mayinga and Kikwit), SEBOV (Boniface), CIEBOV (Cote d'Ivoire), BEBOV, and REBOV (Pennsylvania) strains were used in this study. These viruses were propagated in Vero E6 cells, and viral RNAs were extracted from 250 μl aliquots of culture supernatants using TRIzol-LS reagent (Invitrogen Co., Carlsbad, CA) according to the manufacturer's instructions. The extracted RNA was dissolved in 20 μl of nuclease-free distilled water. All infectious materials were handled in the biosafety level 4 facility of the National Microbiology Laboratory, Public Health Agency of Canada. Lassa virus, hantavirus, dengue 2 virus, and leptospira interrogans RNAs were used as specificity controls because of the similarity of disease symptoms and/or potential endemic area shared with filoviruses.

As shown in Fig. 1A, NP gene fragments of 5 MARV strains and 6 EBOV strains were amplified similarly as 594 bp products by the NP primer combination designed in this study. Nucleotide sequences of all the products were determined and identified as those derived from the respective template strains (data not shown). There was no nonspecific amplification of the Lassa virus and hantavirus RNAs tested. Furthermore, assays using FiloNP-Fm and FiloNP-Rm or FiloNP-Fe and FiloNP-Re primer combinations amplified separately MARV and EBOV RNAs, respectively (Fig. 1B), demonstrating the usefulness of these primer sets in differentiating between MARV and EBOV strains. In contrast, the primers published previously, FILO-A and FILO-B, failed to detect LVMARV Ravn, CIEBOV Cote d'Ivoire, and REBOV Pennsylvania strains (Fig. 1A). The lower stability of the primer match of FILO-A and FILO-B than NP primers, as seen in the alignments between primers and virus genomes, likely influenced the efficiency of amplification (Fig. 2).

To determine the sensitivity of the RT-PCR assay using NP primers, viral RNAs derived from supernatants of samples infected LVMARV strain Angola #368 (approximately 10^7 plaque-forming units (PFU)/ml) (Geisbert et al., 2007), and ZEBOV strain Mayinga (approximately 10^7 focus forming units (FFU)/ml), were diluted serially 10-fold in nuclease-free distilled water, and used as templates for amplification. The detection limits for LVMARV strain

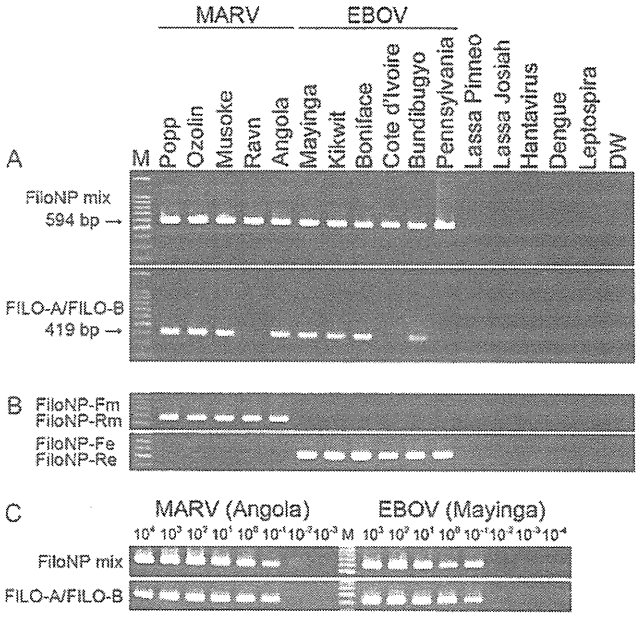

Fig. 1. Specificity and sensitivity of RT-PCR for the detection of MARV and EBOV. (A) Filovirus NP gene fragments were amplified by RT-PCR using a mixture of 4 primers, FiloNP-Fm, FiloNP-Rm, FiloNP-Fe, and FiloNP-Re (upper panel), or FILO-A and FILO-B (lower panel). Lassa virus (strains Pinneo and Josiah), hantavirus (species Dobraba, strain Slovenia), dengue 2 virus (strain VNHCM18-C/02), and leptospira interrogans (serovar Manilae, strain UP-MMC-NIID) RNAs were used to verify the specificity of the RT-PCR. Amplification of these control RNAs by RT-PCR was confirmed by using specific primers for the respective pathogens (data not s tilled water (DW) was used as a negative control. Data independent experiments. (B) MARV and EBOV NP genes Fm and FiloNP-Rm (upper panel) and FiloNP-Fe and FiloN sets, respectively. Lassa virus and hantavirus RNAs were ficity of the RT-PCR. Data are representative of two independent experiments. (C) Tenfold serial dilutions of RNA derived from LVMARV, strain Angola (left) and ZEBOV, strain Mayinga (right) were analyzed; approximate virus titers (PFU for strain Angola and FFU for strain Mayinga) are shown at the top of the panel. Primers FiloNP-Fm, FiloNP-Rm, FiloNP-Fe, and FiloNP-Re (upper panel) and FILO-A and FILO-B (lower panel) were used for amplification. Data are representative of three independent experiments. Lane M: 100-bp DNA ladder.

Angola #368, and ZEBOV strain Mayinga were approximately 10^{-2} to 10^{-1} PFU or FFU/reaction (Fig. 1C) and thus equivalent to the reported sensitivity for the universal primers designed previously (i.e. FILO-A and FILO-B). Although the RT-PCR may not be more sensitive than the TaqMan RT-PCR (Weidmann et al., 2004) and RT-LAMP (Kurosaki et al., 2007, 2010) established previously, the simplicity and cross-reactivity among all known filovirus strains provides an advantage for rapid diagnostics in reference centers and field settings.

Finally, the applicability of RT-PCR using NP primers to *in vivo* diagnostics was studied. Total RNA was extracted from 100 μl of a 10% (w/v) spleen homogenate derived from mice infected with mouse-adapted ZEBOV (titer approximately 10^7 FFU/g) (Ebihara et al., 2006) by using TRIzol-LS reagent (Invitrogen Co.) according to the manufacturer's instructions. The extracted RNA, dissolved in 30 μl of nuclease-free distilled water, was diluted serially 10-fold in nuclease-free distilled water and used as a template. Viral gene fragments were amplified successfully with the detection limit of approximately 10^{-3} FFU/reaction (Fig. 3A), demonstrating that the sensitivity of the RT-PCR assay using NP primers was equivalent to that of the RT-PCR using FILO-A and FILO-B reported previously (Sanchez et al., 1999). Subsequently, whole-blood samples from Marburg hemorrhagic fever cases in Angola in 2004/05 (World Health Organization, 2005) were analyzed. Total RNA was extracted from 100 μl of patient blood samples and dissolved in 10 μl of

Table 1
Primers used in this study.

Primer	Sequence (5′–3′)	Target gene (position)	Product size	Reference strain (accession no. [a])	Reference
FiloNP-Fm	TGGCTTACYACAGGYCACATGAAAGT	MARV NP (620–645)	594 bp	MARV Musoke (NC_001608)	This study
FiloNP-Rm	GTGTGTGATTTCAGTTTTYTGGAGGTGGAA	MARV NP (1213–1184)			
FiloNP-Fe	TGGCAATCAGTDGGACACATGATGGT	EBOV NP (1040–1065)	594 bp	EBOV Mayinga (NC_002549)	This study
FiloNP-Re	GAAGCTGATTTCRTTCTTYTTCTGATGGAA	EBOV NP (1633-1604)			
FILO-A	ATCGGAATTTTTCTTTCTCATT	Filovirus L (13123–13144)	419 bp	MARV Musoke (NC_001608)	Sanchez et al. (1999)
FILO-B	ATGTGGTGGGTTATAATAATCACTGACATG	Filovirus L (13541–13512)			

[a] Accession no. indicates Genbank accession number of reference sequence.

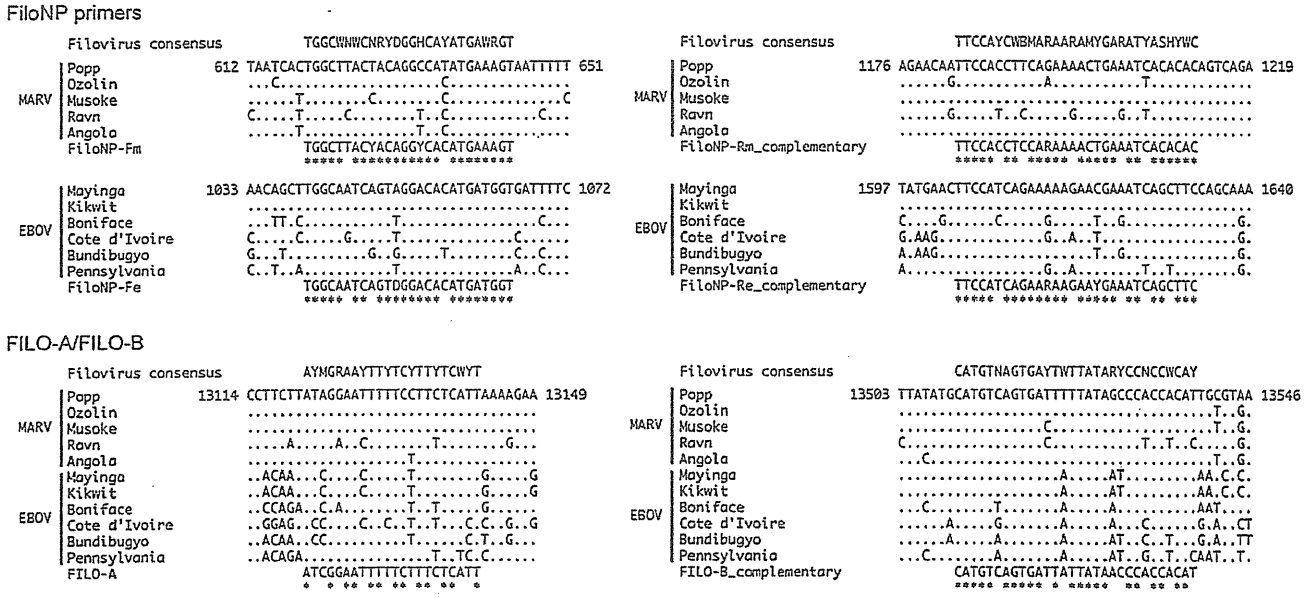

Fig. 2. Alignment of filovirus NP and L gene sequences and primer sequences used in this study. Reverse primers are shown as complementary sequences. Dots indicate the positions identical to LVMARV strain Popp, or ZEBOV strain Mayinga sequences. The numbers on the left and right indicate the respective nucleotide positions in the Popp and Mayinga strain genome sequences. Asterisks indicate the positions matching the primer sequences. Genbank accession numbers of the nucleotide sequences used in this study are Z29337 (Popp), AY358025 (Ozolin), NC_001608 (Musoke), EF446131 (Ravn), DQ447656 (Angola), NC_002549 (Mayinga), AY354458 (Kikwit), FJ968794 (Boniface), FJ217162 (Cote d'Ivoire), FJ217161 (Bundibugyo), and AY769362 (Pennsylvania).

nuclease-free distilled water. Specific amplification of MARV NP gene sequences by the NP primer set was confirmed in all the samples tested, as with the primer set of FILO-A and FILO-B reported previously (Fig. 3B), demonstrating the applicability of this assay to human diagnostics.

In this study, NP-gene-specific primers were designed. NP transcripts were detected *in vitro* as early as 7 h after infection and the number of NP transcript copies was abundant, in contrast to the much lower copy numbers of RNA transcripts derived from the L gene (Sanchez and Kiley, 1987). Thus, this RT-PCR assay using primer sets targeting the NP gene is expected to be more sensitive than those based on L-gene-specific primers to detect cell-associated filovirus RNA transcripts in infected primary target cells such as peripheral monocytes in the early stage of infection. The

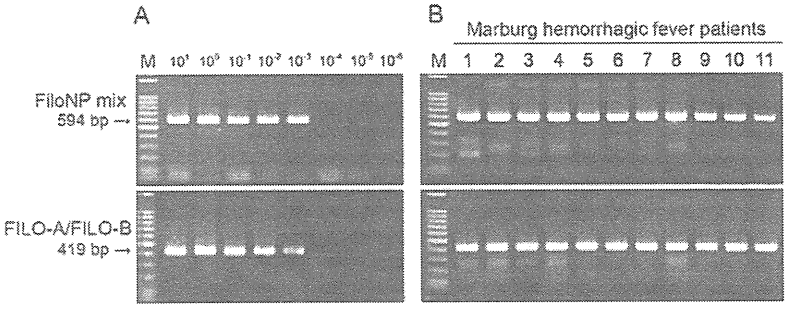

Fig. 3. Detection of EBOV and MARV in experimental animal and human specimens. The NP gene fragments were amplified by RT-PCR using a combination of 4 primers, FiloNP-Fm, FiloNP-Rm, FiloNP-Fe, and FiloNP-Re (upper panels), or FILO-A and FILO-B (lower panels). (A) Tenfold serial dilutions of RNA extracted from ZEBOV-infected mouse spleen were used as templates; approximate virus titers (FFU) used in each reaction are shown at the top of the panel. Data are representative of three independent experiments. (B) MARV-infected human blood specimens obtained during the 2004/05 Marburg hemorrhagic fever outbreak in Angola were analyzed for the presence of MARV RNA. Blood collection from humans during the outbreak in Angola was approved under a special response protocol established between the World Health Organization and national authorities. Lane M: 100-bp DNA ladder.

broad cross-reactivity of RT-PCR with the NP primers designed in this study compared to the ones reported previously will enhance filovirus PCR diagnostics and thus provide a novel tool for public health and biodefense. This combined with its simplicity will also improve ecological and epidemiological field studies in regions with poor infrastructure in Central Africa.

Acknowledgments

We thank Aiko Ohnuma for technical assistance and Kim Barrymore for editing the manuscript. We also thank the Special Pathogens Branch, Centers for Disease Control and Prevention, and Dr. Jiro Arikawa and Dr. Kumiko Yoshimatsu (Hokkaido University), Dr. Kouichi Morita (Nagasaki University), and Dr. Nobuo Koizumi (National Institute of Infectious Diseases) for providing the *Bundibugyo ebolavirus* isolate, hantavirus, dengue 2 virus, and leptospira RNAs, respectively. This work was supported by a grant-in-aid from the Ministry of Health, Labor and Welfare of Japan, and in part by the Program of Founding Research Centers for Emerging and Reemerging Infectious Diseases and the Global COE Program "Establishment of International Collaboration Centers for Zoonosis Control" from the Ministry of Education, Culture, Sports, Science, and Technology, Japan. In addition, the study was supported by the National Microbiology Laboratory of the Public Health Agency of Canada, and the Division of Intramural Research, National Institute of Allergy and Infectious Diseases, National Institute of Health.

References

Centers for Disease Control Prevention, 2009. Imported case of Marburg hemorrhagic fever – Colorado, 2008. MMWR Morb. Mortal. Wkly. Rep. 58, 1377–1381.

Centers for Disease Control and Prevention, 2010a. Known cases and outbreaks of Ebola hemorrhagic fever, in chronological order. Available at: http://www.cdc.gov/ncidod/dvrd/spb/mnpages/dispages/ebola/ebolatable.htm.

Centers for Disease Control and Prevention, 2010b. Known cases and outbreaks of Marburg hemorrhagic fever, in chronological order. Available at: http://www.cdc.gov/ncidod/dvrd/spb/mnpages/dispages/marburg/marburgtable.htm.

Drosten, C., Gottig, S., Schilling, S., Asper, M., Panning, M., Schmitz, H., Gunther, S., 2002. Rapid detection and quantification of RNA of Ebola and Marburg viruses, Lassa virus, Crimean-Congo hemorrhagic fever virus, Rift Valley fever virus, dengue virus, and yellow fever virus by real-time reverse transcription-PCR. J. Clin. Microbiol. 40, 2323–2330.

Ebihara, H., Takada, A., Kobasa, D., Jones, S., Neumann, G., Theriault, S., Bray, M., Feldmann, H., Kawaoka, Y., 2006. Molecular determinants of Ebola virus virulence in mice. PLoS Pathog. 2, e73.

Feldmann, H., Geisbert, T.W., Jahrling, P.B., 2004. Filoviridae. In: Fauquet, C.M., Mayo, M.A., Maniloff, J., Desselberger, U., Ball, L.A. (Eds.), Virus Taxonomy: Eighth Report of the International Committee on Taxonomy of Viruses. Elsevier Academic Press, London, pp. 645–653.

Feldmann, H., Jones, S., Klenk, H.D., Schnittler, H.J., 2003. Ebola virus: from discovery to vaccine. Nat. Rev. Immunol. 3, 677–685.

Geisbert, T.W., Daddario-DiCaprio, K.M., Geisbert, J.B., Young, H.A., Formenty, P., Fritz, E.A., Larsen, T., Hensley, L.E., 2007. Marburg virus Angola infection of rhesus macaques: pathogenesis and treatment with recombinant nematode anticoagulant protein c2. J. Infect. Dis. 196 (Suppl. 2), S372–381.

Gibb, T.R., Norwood Jr., D.A., Woollen, N., Henchal, E.A., 2001. Development and evaluation of a fluorogenic 5′-nuclease assay to identify Marburg virus. Mol. Cell. Probes 15, 259–266.

Kurosaki, Y., Grolla, A., Fukuma, A., Feldmann, H., Yasuda, J., 2010. Development and evaluation of the simple diagnostic assay for Marburg virus using reverse transcription-loop-mediated isothermal amplification method. J. Clin. Microbiol. 48, 2330–2336.

Kurosaki, Y., Takada, A., Ebihara, H., Grolla, A., Kamo, N., Feldmann, H., Kawaoka, Y., Yasuda, J., 2007. Rapid and simple detection of Ebola virus by reverse transcription-loop-mediated isothermal amplification. J. Virol. Methods 141, 78–83.

Sanchez, A., Geisbert, T.W., Feldmann, H., 2006. Filoviridae: Marburg and Ebola viruses. In: David, M.K., Peter, M.H. (Eds.), Fields Virology. Lippincott Williams and Wilkins, a Wolters Kluwer Business, Philadelphia, pp. 1409–1448.

Sanchez, A., Kiley, M.P., 1987. Identification and analysis of Ebola virus messenger RNA. Virology 157, 414–420.

Sanchez, A., Ksiazek, T.G., Rollin, P.E., Miranda, M.E., Trappier, S.G., Khan, A.S., Peters, C.J., Nichol, S.T., 1999. Detection and molecular characterization of Ebola viruses causing disease in human and nonhuman primates. J. Infect. Dis. 179 (Suppl. 1), S164–S169.

Timen, A., Koopmans, M.P., Vossen, A.C., van Doornum, G.J., Gunther, S., van den Berkmortel, F., Verduin, K.M., Dittrich, S., Emmerich, P., Osterhaus, A.D., Dissel, J.T., Coutinho, R.A., 2009. Response to imported case of Marburg hemorrhagic fever, the Netherland. Emerg. Infect. Dis. 15, 1171–1175.

Towner, J.S., Sealy, T.K., Khristova, M.L., Albarino, C.G., Conlan, S., Reeder, S.A., Quan, P.L., Lipkin, W.I., Downing, R., Tappero, J.W., Okware, S., Lutwama, J., Bakamutumaho, B., Kayiwa, J., Comer, J.A., Rollin, P.E., Ksiazek, T.G., Nichol, S.T., 2008. Newly discovered Ebola virus associated with hemorrhagic fever outbreak in Uganda. PLoS Pathog. 4, e1000212.

Weidmann, M., Muhlberger, E., Hufert, F.T., 2004. Rapid detection protocol for filoviruses. J. Clin. Virol. 30, 94–99.

World Health Organization, 1997. Ebola haemorrhagic fever. A summary of the outbreak in Gabon. Wkly. Epidemiol. Rec. 72, 7–8.

World Health Organization, 2005. Marburg haemorrhagic fever, Angola. Wkly. Epidemiol. Rec. 80, 158–159.

CLINICAL AND VACCINE IMMUNOLOGY, Nov. 2010, p. 1723–1728 Vol. 17, No. 11
1556-6811/10/$12.00 doi:10.1128/CVI.00170-10

Enzyme-Linked Immunosorbent Assay for Detection of Filovirus Species-Specific Antibodies▽

Eri Nakayama,[1] Ayaka Yokoyama,[1] Hiroko Miyamoto,[1] Manabu Igarashi,[1] Noriko Kishida,[2] Keita Matsuno,[1] Andrea Marzi,[3] Heinz Feldmann,[3] Kimihito Ito,[1] Masayuki Saijo,[4] and Ayato Takada[1]*

Department of Global Epidemiology, Hokkaido University Research Center for Zoonosis Control, Sapporo, Hokkaido, Japan[1]; Laboratory of Influenza Virus Surveillance, Center for Influenza Virus Research, National Institute of Infectious Diseases, Tokyo, Japan[2]; Laboratory of Virology, Division of Intramural Research, National Institute of Allergy and Infectious Diseases, National Institutes of Health, Rocky Mountain Laboratories, Hamilton, Montana[3]; and Department of Virology 1, National Institute of Infectious Diseases, Tokyo, Japan[4]

Received 16 April 2010/Returned for modification 29 June 2010/Accepted 23 August 2010

Several enzyme-linked immunosorbent assays (ELISAs) for the detection of filovirus-specific antibodies have been developed. However, diagnostic methods to distinguish antibodies specific to the respective species of filoviruses, which provide the basis for serological classification, are not readily available. We established an ELISA using His-tagged secreted forms of the transmembrane glycoproteins (GPs) of five different Ebola virus (EBOV) species and one Marburg virus (MARV) strain as antigens for the detection of filovirus species-specific antibodies. The GP-based ELISA was evaluated by testing antisera collected from mice immunized with virus-like particles as well as from humans and nonhuman primates infected with EBOV or MARV. In our ELISA, little cross-reactivity of IgG antibodies was observed in most of the mouse antisera. Although sera and plasma from some patients and monkeys showed notable cross-reactivity with the GPs from multiple filovirus species, the highest reactions of IgG were uniformly detected against the GP antigen homologous to the virus species that infected individuals. We further confirmed that MARV-specific IgM antibodies were specifically detected in specimens collected from patients during the acute phase of infection. These results demonstrate the usefulness of our ELISA for diagnostics as well as ecological and serosurvey studies.

Ebola virus (EBOV) and Marburg virus (MARV) belong to the family *Filoviridae* and cause severe hemorrhagic fever in primates (20). While MARV consists of a single species, *Lake Victoria marburgvirus*, four distinct EBOV species are known: *Zaire ebolavirus* (ZEBOV), *Sudan ebolavirus* (SEBOV), *Côte d'Ivoire ebolavirus* (CIEBOV), and *Reston ebolavirus* (REBOV). The phylogenetically distinct *Bundibugyo ebolavirus* (BEBOV) was recently identified in Uganda and was proposed to be a new species of EBOV (Fig. 1) (31).

EBOV and MARV are filamentous, enveloped, single-stranded, negative-sense RNA viruses. The virus genome encodes seven structural proteins, nucleoprotein (NP), polymerase cofactor (VP35), matrix protein (VP40), glycoprotein (GP), replication-transcription protein (VP30), minor matrix protein (VP24), and RNA-dependent RNA polymerase (L). EBOV also expresses at least one secreted nonstructural glycoprotein (sGP) (20). GP is responsible for receptor binding and fusion of the viral envelope with host cell membranes (11, 22, 35) and has an important role in the pathogenesis of filovirus infection (3, 23, 36). GP is the main target of neutralizing antibodies, and most of the known ZEBOV-specific monoclonal antibodies (MAbs) show little cross-reactivity to other filovirus species (24, 27, 34).

Serological diagnostic methods based on enzyme-linked immunosorbent assays (ELISAs) using the recombinant EBOV and MARV NP antigens have been developed to detect filovirus-specific antibodies (5, 17). Using a ZEBOV NP antigen, NP-specific antibodies were broadly detected in animals infected with ZEBOV, SEBOV, CIEBOV, or REBOV (17), indicating strong cross-reactivity among EBOV species. It is predicted, however, that the antibody response to GP is more species specific due to the larger genetic variability with this protein, which is supposed to be the main target of the host humoral immune response. Therefore, in this study we developed a filovirus species-specific ELISA using recombinant GP antigens to serologically distinguish filovirus species.

MATERIALS AND METHODS

Plasmids. Viral RNA extracted from the supernatant of Vero E6 cells infected with ZEBOV, SEBOV, CIEBOV, BEBOV, REBOV, or MARV strain Angola was used for the cloning of the respective GP cDNAs lacking the transmembrane domain and cytoplasmic tail. The cDNAs of truncated EBOV and MARV GPs with a C-terminal histidine (His) tag (His-EBOV-GP and His-MARV-GP, respectively) were cloned into a pATX vector. Finally, the cDNA fragments of His-EBOV-GP and His-MARV-GP were inserted into the mammalian expression vector pCAGGS/MCS, which contains the chicken β-actin promoter (13). All clones were confirmed by sequencing prior to expression.

MAbs. Hybridoma cells producing EBOV GP-specific MAb ZGP42/3.7 (IgG1) (24, 26), which recognizes a linear epitope on GP comprising the sequence GEWAFWENKKN, and MARV GP-specific MAb AGP127-8 (IgG1) were grown in Dulbecco's modified Eagle's medium (DMEM) (Sigma) and RPMI medium (Sigma), respectively, supplemented with fetal calf serum (FCS) and antibiotics. Mouse ascites were obtained by a standard procedure, and MAbs were purified from ascites fluid using protein A-agarose columns (Bio-Rad). The S139/1 monoclonal antibody (IgG2a), which binds to the hemagglutinin of influenza A viruses (37), was used as a negative control.

* Corresponding author. Mailing address: Department of Global Epidemiology, Hokkaido University Research Center for Zoonosis Control, Kita-20, Nishi-10, Kita-ku, Sapporo 001-0020, Japan. Phone: 81-11-706-9502. Fax: 81-11-706-7310. E-mail: atakada@czc.hokudai.ac.jp.

▽ Published ahead of print on 22 September 2010.

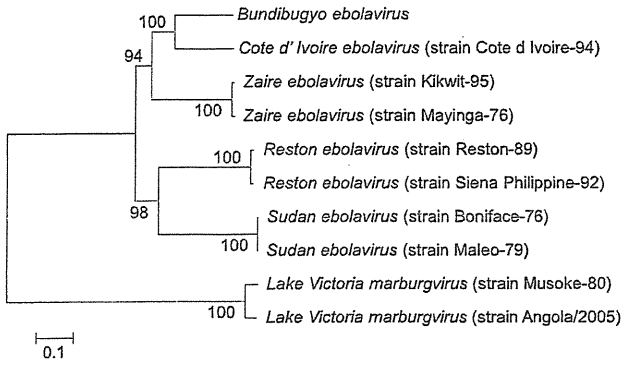

FIG. 1. Phylogenetic analysis of filovirus GP amino acid sequences. The phylogenetic tree was constructed by using the neighbor-joining method. For the construction of this tree, we used 10 GP amino acid sequences, each comprising a whole GP amino acid sequence. Numbers at branch points indicate bootstrap values (1,000 replicates).

Sera and plasma. Five-week-old female BALB/c mice were immunized twice intraperitoneally with 100 μg virus-like particles (VLPs) (14, 21) in 3-week intervals, and the serum samples were collected 7 to 10 days after the second immunization. Convalescent-phase plasma samples were collected from cynomolgus macaques vaccinated and/or infected with EBOV as described previously (27). ZEBOV convalescent-phase human plasma (patients 2 to 7) and serum (patients 1 and 8) samples were obtained 51 to 135 days after the onset of ZEBOV infection during the 1995 outbreak in Kikwit, Democratic Republic of the Congo (25). SEBOV convalescent-phase patient serum samples (patients 9 and 10) were collected about 2 months after onset during the Ebola hemorrhagic fever outbreaks in Uganda in 2000 associated with SEBOV (2). These EBOV-infected human samples were kindly provided by T. G. Ksiazek (Centers for Disease Control and Prevention). MARV-infected human blood samples (patients 11 to 21) were collected within a few days after the onset of symptoms from admitted patients from the 2004-2005 outbreak in Angola (29). Blood collections during outbreak investigations were approved under the special response protocol established between the World Health Organization and national authorities.

Expression and purification of His-EBOV-GP and His-MARV-GP. Human epithelial kidney 293T cells cultured in high-glucose DMEM containing 10% FCS and antibiotics were transfected with pCAGGS vectors expressing His-EBOV-GP (pCHis-ZEBOV-GP, pCHis-SEBOV-GP, pCHis-CIEBOV-GP, pCHis-BEBOV-GP, or pCHis-REBOV-GP) or His-MARV-GP (pCHis-MARV-GP) using TransIT LT1 (Mirus). Forty-eight hours after transfection, the supernatants were collected, and the recombinant GPs were purified by using the Ni-nitrilotriacetic acid (NTA) purification system (Invitrogen) according to the manufacturer's instructions. The majority of contaminant protein was removed with wash buffer containing 15 mM imidazole. Finally, bound proteins were collected with elution buffer containing 250 mM imidazole. To monitor inevitable nonspecific reactions (i.e., nonspecific antibodies) to FCS-derived impurities in each GP preparation, control antigens (FCS-derived proteins nonspecifically bound to the Ni beads) were prepared by using the Ni-NTA column under the same conditions. The eluted protein was concentrated by using Amicon Ultra 4 spin columns (Millipore) and dialyzed against phosphate-buffered saline (PBS) at 4°C overnight. Purified His-EBOV-GP and His-MARV-GP were analyzed by sodium dodecyl sulfate-polyacrylamide gel electrophoresis (SDS-PAGE) and stained with Coomassie brilliant blue. Western blotting was performed by using ZGP42/3.7, AGP127-8, and anti-His MAbs (Covance).

Antigens prepared from cell lysates and VLPs. Membrane lysates of 293T cells transfected with pCAGGS expressing full-length GP were prepared by using the Mem-PER eukaryotic membrane protein extraction reagent kit (Pierce) according to the manufacturer's instructions. To generate VLPs, 293T cells were transfected with plasmids expressing major viral structural proteins, GP, NP, and VP40 (10, 33). After 48 h, supernatants were overlaid on 25% sucrose and ultracentrifuged at 28,000 × *g* at 4°C for 1.5 h. The VLPs were recovered from the pellet and disrupted with 0.05% Triton X-100 in the presence of 30 mM potassium chloride for the use of ELISA antigens. The GP amounts in the membrane lysates and VLPs were quantified by Western blotting using MAb ZGP42/3.7 or AGP127-8, and the GP concentrations of each preparation were calculated based on the standard band intensities provided by known concentrations of His-GP. Membrane lysates or supernatants of 293T cells transfected with empty pCAGGS vectors were used to prepare control antigens for ELISA using cell lysates or VLPs, respectively.

ELISA. ELISA plates (Nunc Maxisorp) were coated with the GP antigens (100 ng of GP/50 μl/well) or control antigens in PBS at 4°C overnight and then washed with PBS containing 0.05% Tween 20 (PBST). Unspecific binding of the antibodies was avoided by blocking with 3% skim milk (150 μl/well) for 2 h at room temperature. Monkey plasma samples were preincubated with 2% FCS to absorb antibodies to FCS components, since they were exposed to FCS by the injection of the vaccines or viruses diluted in DMEM containing FCS. After washing three times with PBST, 50 μl of appropriately diluted serum or plasma samples or the GP-specific MAb in PBST containing 1% skim milk was added and incubated for 1 h at room temperature. After washing three times with PBST, the bound antibodies were detected by using the following secondary antibodies conjugated with horseradish peroxidase diluted in 1% skim milk in PBST: goat anti-mouse IgG (Jackson ImmunoResearch), goat anti-monkey IgG (Rockland), goat anti-human IgG (Jackson ImmunoResearch), or donkey anti-human IgM (Jackson ImmunoResearch). After incubation for 1 h at room temperature and three PBST washes, 50 μl of 3,3′,5,5′-tetramethylbenzidine (Sigma) was added to each well, and the mixture was incubated for 15 min at room temperature. The reaction was stopped by adding 1 N sulfuric acid to the mixture, and the optical density (OD) at 450 nm was measured.

Phylogenetic analysis. Phylogenetic analysis was based on whole amino acid sequences of filovirus GPs. The sequences were analyzed by using GENETYX (Genetyx Corp., Japan) for Windows software, version 7. A phylogenetic tree was constructed by using the neighbor-joining bootstrap method (1,000 replicates) in MEGA 4.0 software (28). Amino acid sequences of ZEBOV strain Mayinga-76, ZEBOV strain Kikwit-95, SEBOV strain Boniface-76, SEBOV strain Maleo-79, CIEBOV strain Côte d'Ivoire-94, BEBOV, REBOV strain Reston-89, REBOV strain Siena Philippine-92, MARV strain Musoke-80, and MARV strain Angola/2005 used in phylogenetic analyses were obtained from GenBank under accession numbers Q05320, P87666, Q66814, Q66798, Q66810, ACI28624, Q66799, Q89853, P35253, and Q1PD50, respectively.

Statistical analyses. OD values higher than 3 standard deviations above the averages of negative-control samples at a 1:100 dilution were considered positive. To test the specificity of each reaction, ELISA data (i.e., OD values) were analyzed by using one-way analysis of variance (ANOVA). The differences between OD values were compared by using the two-sided *t* test with the Bonferroni-Holm correction for multiple comparisons (4). All statistical analyses were performed with the computer program R (version 2.2.8).

RESULTS

Expression and purification of recombinant EBOV and MARV GPs. The expression and secretion of His-EBOV-GP and His-MARV-GP in the supernatants of 293T cells transfected with a plasmid encoding His-GP were confirmed by immunoblotting using anti-GP and anti-His MAbs (data not shown). These recombinant GPs were purified as described in Materials and Methods. All purified His-GPs were detected by SDS-PAGE and immunoblotting using anti-GP and anti-His MAbs as prominent protein bands of the predicted size of the transmembrane anchor-minus EBOV and MARV GPs (Fig. 2). These purified GPs were used as antigens for the ELISA described in the following experiments.

Sensitivity of the GP-based ELISA. The sensitivity of the purified GP-based ELISA was tested by using anti-EBOV-GP MAb ZGP42/3.7 and anti-MARV-GP MAb AGP127-8. Serial 10-fold dilutions of the antibodies (10^{-5} to 10^{2} μg/ml) were prepared, and the reactivity to each GP antigen was examined (Fig. 3a to c). The negative-control MAb, S139/1, did not bind to any His-GPs in the ELISA. At concentrations ranging from 0.1 μg/ml to 100 μg/ml, ZGP42/3.7 reacted with all His-EBOV-GPs but not His-MARV-GP, whereas AGP127-8 reacted specifically with His-MARV-GP but not any of the His-EBOV-GPs. The detection limit for specific antibodies using this assay

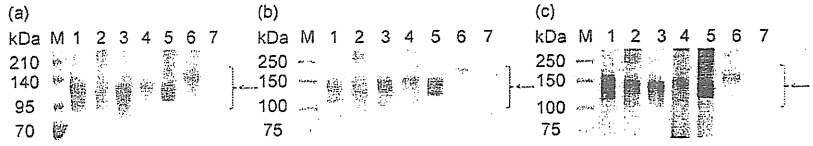

FIG. 2. Identification and characterization of purified His-GPs. (a) His-EBOV-GP and His-MARV-GP were analyzed by 8% SDS-PAGE and stained with Coomassie brilliant blue. (b and c) Immunoblotting of purified His-GPs was performed by using MAbs to EBOV (ZGP42/3.7) and MARV GPs (AGP127-8) (b) and His tags (c). Arrows indicate the locations of the His-GPs. The protein bands represent His-ZEBOV-GP (lane 1), His-SEBOV-GP (lane 2), His-CIEBOV-GP (lane 3), His-BEBOV-GP (lane 4), His-REBOV-GP (lane 5), and His-MARV-GP (lane 6). Lane 7 shows FCS-derived proteins used as a control antigen (see Materials and Methods).

was approximately 0.01 to 0.1 μg/ml. On the other hand, ELISA using membrane lysates of GP-transfected cells or VLPs under similar conditions with the GP-based ELISA showed lower sensitivity, except for the Angola serum and VLP combination (Fig. 3d to i). This is most likely due to the interference by the residual detergent and/or irrelevant proteins in the lysates and VLP antigen preparations.

Specificity of the GP-based ELISA. Next, the species specificity of the ELISA was assessed by testing the antisera of mice immunized with VLP containing the respective EBOV and MARV GPs. We found that species-specific IgG antibodies were clearly detected in these mouse antisera (Fig. 4a to f). All the anti-EBOV IgG antibodies in the sera showed low reactivity to heterologous EBOV GPs, and no cross-reactivity to MARV GP was found (Fig. 4a to e). Similarly, anti-MARV VLP serum antibodies reacted to MARV GP but not to EBOV GPs (Fig. 4f). These results indicated that this purified GP-based ELISA sufficiently detected filovirus species-specific antibodies. On the other hand, the VLP-based ELISA was less sensitive and detected more appreciable cross-reactive antibodies in some of the mouse sera, likely specific to NP and VP40, than the purified GP-based ELISA (Fig. 4g to i).

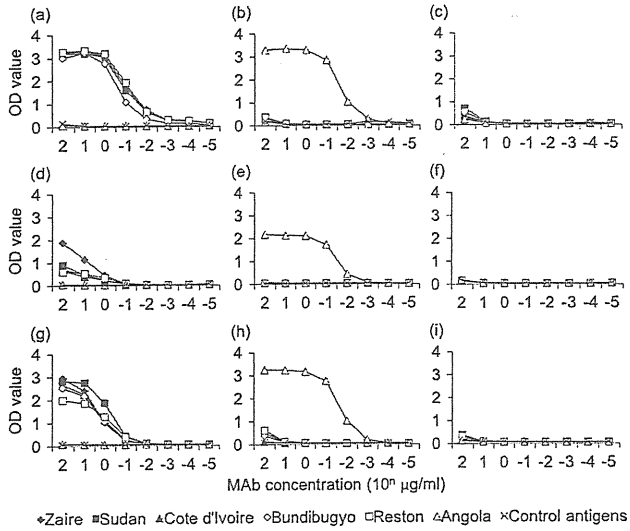

FIG. 3. Sensitivity of ELISAs. His-GPs (a, b, and c), GP-expressing cell lysates (d, e, and f), and VLP (g, h, and i) were used as antigens. The GP amounts were standardized by Western blotting as described in Materials and Methods. Serial 10-fold dilutions of MAbs to EBOV (a, d, and g) and MARV (b, e, and h) were prepared and tested. S139/1 (specific to influenza virus hemagglutinin) was used as a negative-control antibody (c, f, and i).

Analysis of clinical samples in the GP-based ELISA. To further confirm the specificity of our ELISA, we used convalescent-phase plasma samples obtained from monkeys experimentally infected with ZEBOV or SEBOV (Fig. 5). The cutoff OD values (i.e., the mean plus 3 standard deviations of the five negative serum samples) were 0.23, 0.22, 0.29, 0.22, 0.17, 0.20, and 0.13 for His-ZEBOV-GP, His-SEBOV-GP, His-CIEBOV-GP, His-BEBOV-GP, His-REBOV-GP, His-MARV-GP, and control antigens, respectively. According to these thresholds, all infected monkey serum samples tested were EBOV antibody positive. We detected IgG antibodies in the ZEBOV-infected monkey plasma with higher reactivity against His-ZEBOV-GP than against any heterologous GP antigens. Although IgG antibodies in the SEBOV-infected monkey plasma showed binding to all His-EBOV-GPs, the highest reactivity was observed with the homologous antigen His-SEBOV-GP. Neither of these plasma antibodies reacted with MARV GP.

We then examined IgG antibody levels in serum or plasma derived from ZEBOV-, SEBOV-, and MARV-infected patients (Fig. 6a). The cutoff OD values obtained from the five negative-control sera for IgG antibodies were 0.20, 0.17, 0.24, 0.18, 0.14, 0.27, and 0.23 for His-ZEBOV-GP, His-SEBOV-GP, His-CIEBOV-GP, His-BEBOV-GP, His-REBOV-GP, His-MARV-GP, and control antigens, respectively. For most of the samples tested, IgG antibodies to homologous GP antigens were detected with the highest reactivity (Fig. 6a). All of the samples derived from ZEBOV-infected patients cross-reacted with His-CIEBOV-GP and His-BEBOV-GP antigens, whereas only one of the SEBOV-infected human samples (sample 9) showed cross-reactivity with His-MARV-GP. Overall, the level of cross-reactivity was consistent with the phylogenetic relationship among EBOV species (Fig. 1). On the other hand, for most of the samples from patients infected with MARV Angola, IgG antibodies to His-MARV-GP were specifically detected, except for specimen 17, which showed no IgG response to any GP. Interestingly, IgG antibodies detected in specimen 11 showed remarkable cross-reactivity with the heterologous antigens His-CIEBOV-GP and His-BEBOV-GP.

We next evaluated whether GP-specific IgM antibodies could be detected in the patient serum or plasma samples using the GP-based ELISA (Fig. 6b). The cutoff values for IgM ELISA were 0.23, 0.32, 0.31, 0.28, 0.30, 0.22, and 0.36 for His-ZEBOV-GP, His-SEBOV-GP, His-CIEBOV-GP, His-BEBOV-GP, His-REBOV-GP, His-MARV-GP, and control

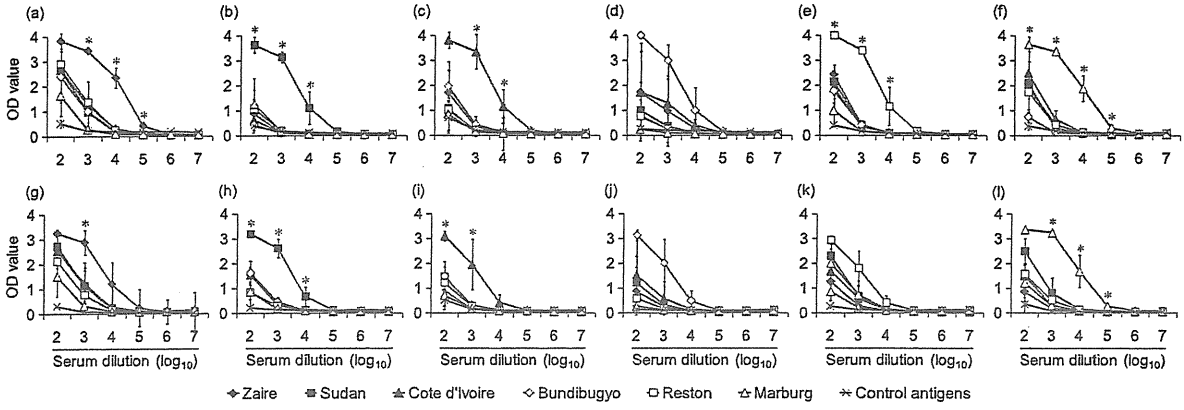

FIG. 4. IgG antibodies detected in mouse antisera. Serial 10-fold dilutions of anti-ZEBOV (a and g), anti-SEBOV (b and h), anti-CIEBOV (c and i), anti-BEBOV (d and j), anti-REBOV (e and k), and anti-MARV (f and l) sera obtained from mice immunized with EBOV and MARV VLPs were tested for IgG antibodies reacting with His-GPs (a, b, c, d, e, and f) and VLPs (g, h, i, j, k, and l). Averages and standard deviations for three mice of each group are shown. Asterisks indicate statistically significant differences in OD values between the homologous antigen and all other antigens ($P < 0.05$).

antigens, respectively. ZEBOV- or SEBOV-specific IgM antibodies were detected only in patients 2, 6, 9, and 10. In contrast, MARV-specific IgM antibodies were detected in 8 out of the 11 specimens derived from MARV Angola-infected patients. No obvious IgM cross-reactivity to heterologous GP antigens was found in these samples.

DISCUSSION

In this study, we established a GP-based ELISA to detect filovirus species-specific antibodies. To date, lysates from Vero E6 cells infected with live EBOV and MARV or recombinant EBOV and MARV NPs have been used as antigens in ELISAs for the detection of filovirus-specific antibodies (5, 7, 17). Since the NPs of EBOV and MARV contain similar amino acid sequences (18), common antibody epitopes seem to be present (12). Indeed, cross-reactivity among all EBOV species was to be expected (16, 17). Therefore, NP antigens may be useful for the detection of genus-specific antibodies but not for the detection of species-specific humoral responses (7, 16, 17).

The heterogeneity of EBOV and MARV GPs has been demonstrated at the genetic level through sequence analyses (17, 19). An ELISA using recombinant ZEBOV GP expressed in a baculovirus-insect cell expression system was reported previously (16), but it is known that the protein glycosylation pathways in insect cells differ from those in mammalian cells (6). This may significantly affect the antigenic properties of filovirus GPs, since large amounts of both N- and O-linked carbohydrate chains are present in GP molecules. To overcome this difficulty, we used mammalian 293T cells for the expression of GP antigens and verified the sensitivity and specificity of GP-based ELISAs. Our results were consistent with a previous study suggesting that anti-EBOV GP antibodies were highly species specific and showed little cross-reactivity to GPs of other EBOV species (27). These findings indicated that most antibodies induced against filovirus GPs recognized

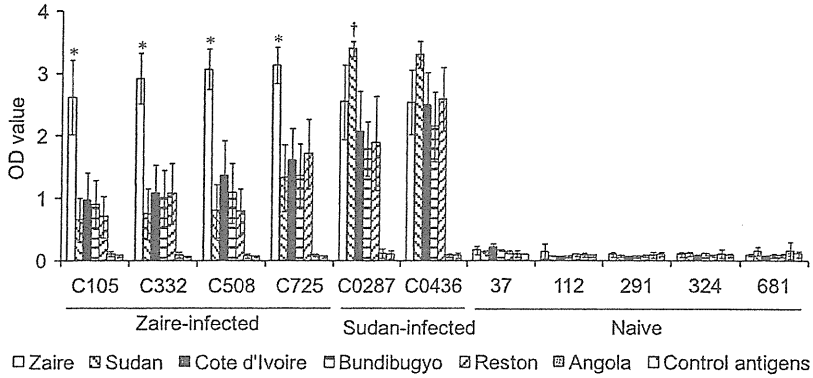

FIG. 5. IgG antibodies detected in experimentally infected monkey plasma by ELISA using His-GPs. Monkeys C105, C332, C508, and C725 were infected with ZEBOV, whereas monkeys C0287 and C0436 were infected with SEBOV. Infected monkey sera were diluted at 1:1,000. Naïve monkey sera were diluted at 1:100. Each bar represents the average and standard deviation of data from three independent experiments. Asterisks indicate statistically significant differences in OD values between the Zaire antigen and all other antigens ($P < 0.05$). The dagger shows statistically different reactions between His-SEBOV-GP and all the other antigens ($P < 0.05$) except His-ZEBOV-GP.